```
Chronology and Erosion rate of the Pinedale glaciation, Colorado Front Range (USA),
1
2
      Inferred from the Sedimentary record of glacial Lake Devlin
3
4
      David P. Dethier, Matthias Leopold, Jörg Völkel, Jan-Pieter Buylaert, Andrew Murray,
      Robert E. Nelson<sup>6</sup>, Richard Madole<sup>7</sup>, Lee B. Corbett<sup>8</sup>, Paul Bierman<sup>8</sup> and Joseph
5
6
      Rosenbaum<sup>9</sup>
7
8
      <sup>1</sup> Department of Geosciences
      Williams College 303 Clark Hall,
9
      Williamstown, Massachusetts 01267, U.S.A.
10
11
      <sup>2</sup> School of Agriculture and Environment, MO79
12
      The University of Western Australia
13
      35 Stirling Highway
14
15
      6009 CRAWLEY, WA Australia
16
      <sup>3</sup> Geomorphology & Soil Science
17
      TUM School of Life Sciences
18
19
      Technical University of Munich Hans-Carl-von-Carlowitz-Platz 2
20
      D-85354 Freising-Weihenstephan, Germany
21
      <sup>4</sup> Department of Physics
22
23
      Technical University of Denmark
24
      DTU Risø campus, Frederiksborgvej 399
      DK-4000 Roskilde, Denmark
25
26
      <sup>5</sup> Nordic Laboratory for Luminescence Dating
27
28
      Department of Geoscience
      Aarhus University
29
      DTU Risø campus, Frederiksborgvej 399
30
31
      DK-4000 Roskilde, Denmark
32
33
      <sup>6</sup> Department of Geology
      Colby College
34
35
      5800 Mayflower Hill
36
      Waterville, Maine 04901-8858, U.S.A.
37
      <sup>7</sup> 3075 Fremont St., Boulder
38
39
      Colorado 80225
40
      <sup>8</sup> Rubenstein School of the Environment and Natural Resources
41
      University of Vermont Burlington, VT 05405
42
43
      <sup>9</sup> 1205 Hastings St., Delta CO 81416
44
```

46 ABSTRACT

Glacial and periglacial sediments and landforms record the chronology of glaciation and amount of Pleistocene erosion during colder periods that added substantially to global sediment budgets and contributed to the global CO2 cycle. The now-drained glacial Lake Devlin, dammed in a Front Range tributary valley by a glacier in the North Branch of Boulder Creek, Colorado, preserves an important sedimentary archive of the c. 32-14 ka Pinedale glaciation, recording both paleoclimate information and an integrated measure of glacial and periglacial erosion rates over a full glacial cycle. Despite rapid erosion of fine-grained deposits after the lake drained, most sediment generated during Pinedale time remains as legacy deposits in the catchment. Geomorphic evidence and dating of glaciolacustrine sediment from surface exposures demonstrate that the c. 30 ka Pinedale glacial advance was nearly as extensive as the local Late Glacial Maximum at ~20 ka. Sedimentary archives dated by <sup>14</sup>C, optically stimulated luminescence and cosmogenic nuclides extend earlier studies (Madole et al., 1973) of pollen and magnetic susceptibility (MS) in cores from the glaciolacustrine deposits of Lake Devlin and of Pinedale climate. Records suggest shortterm warming and biotic change at about 15 ka after ~14 kyr of cold, dry conditions punctuated by MS peaks at ~26.5, 20 and 16.5 ka. Lake Devlin drained catastrophically after ~14 ka, millennia after ice had retreated upvalley from the lateral moraine that dammed the lake. Sediment production during the Pinedale was equivalent to a periglacial and glacial erosion rate of ~70 mm kyr<sup>-1</sup>, several times higher than long-term rates in the adjacent Front Range, but much lower than rates measured where modern glaciers are eroding weak bedrock in zones of rapid rock uplift, such as SSE Alaska. Data from the Lake Devlin basin contribute to contemporary discussions of how glacial erosion influences the global CO<sub>2</sub> cycle.

70

47

48

49

50

51

52

53

54

55

56

57

58

59

60

61

62

63

64

65

66

67

68

69

71

73 INTRODUCTION

74

75

76

77

78

79

80

81

82

83

84

85

86

87

88

89

90

91

92

93

94

95

96

97

98

99

During the most recent glaciation, glacial, periglacial and paraglacial processes mobilized large quantities of sediment from alpine and subalpine catchments (Hallet et al., 1996), likely contributing to increases in silicate weathering (Herman et al. 2013). After the local Last Glacial Maximum (LLGM) between 26.5 and 19.0 thousands of years (ka) (Clark et al. 2009), rapid hemispheric fluctuations of climate, including the Bølling-Allerød warming, Younger Dryas cooling and early Holocene warmth caused glacier retreat, local stillstands and readvances, and redistribution of sediment. Sedimentary archives preserved in marginal basins isolated by ice damming represent a valuable opportunity to explore the timing of regional climate events in the context of global glaciations and to estimate rates of erosion, sediment flux and storage during cold periods, and their contribution the global CO<sub>2</sub> cycle.

Although there is a long history of glacial studies in the western US, the relationship between periods of coldest climate and the extent of glacial advances remains an active area of research (Quirk et al., 2022). During the latest Pleistocene, alpine glaciers and local icefields in the mountains of the western USA grew after about 32 ka and retreated into cirque areas before ~12 ka, a time period named the Pinedale glaciation in the southern Rocky Mountains for the spectacular moraine sequence near Pinedale, Wyoming (Blackwelder, 1915). Some stratigraphic evidence from the southern Rocky Mountains (Pierce et al., 1976; Nelson et al, 1979) and the Sierra and Cascade Ranges (Phillips et al., 1996; Rosenbaum et al., 2012) shows that Pinedale glaciers advanced at ~ 32 ka in areas where the local Last Glacial Maximum (LLGM) occurred about 10 kyr later (Davis et al., 2009; Young et al., 2011; Laabs et al., 2020). The influence of local climate and whether the LLGM, subsequent ice retreat and stillstands were regionally synchronous continues to be debated (e.g. Sweinsberg et al., 2020; Quirk et al., 2022), but the LLGM advances obscured evidence of the early Pinedale. Initiation and termination of the glacial period corresponds with global climate records, perhaps most closely with those of the Asian monsoon (Zhang et al., 2018) and the marine record of the northeastern Pacific (Walczak et al., 2020).

Glacial Lake Devlin (Lake DE), a long-lived ice-marginal lake in the southern Rocky Mountains, is a critical area for reconstructing the history of Pinedale ice advance and retreat and environmental conditions during the most recent glacial cycle (Madole, 1986; Madole, 2010; Dühnforth and Anderson, 2011). Lake Devlin served as a nearly perfect sediment trap for 15 kyr, recording both paleoclimate information and an integrated measure of glacial and periglacial erosion rates over a full glacial cycle. In the early 1970s, Rich Madole and fellow investigators extracted several cores as long as 20 m from Lake Devlin bottom sediment, dated the cores using radiocarbon techniques (Madole, 1986), and used the sediment for sedimentologic, palynologic (Legg and Baker, 1980), and magnetic susceptibility (MS) analysis (Rosenbaum and Larson, 1983). Coring recovered ~14 m of laminated clayey silt and silty clay above 17 m of fluvial and lacustrine sediment that could not be extracted by coring (Madole, 1986). Interpretation of <sup>14</sup>C ages (Madole, 1986; 2010) suggested that the 0.28 km<sup>2</sup> Lake Devlin formed at ~ 30 ka when a Front Range valley glacier and its lateral moraine in the North Boulder Creek (NBC) valley blocked drainage from Caribou Creek, a tributary, and drained catastrophically sometime after ice had retreated upvalley. Cosmogenic exposure ages from bedrock surfaces in adjacent valleys (Ward et al., 2009; Dühnforth and Anderson, 2011) indicate that ice retreat started after 20 ka and ended before 13-12 ka in upvalley cirques. Lake Devlin sediment contains an unusually completely record of the entire Pinedale, which allows us to examine regional glacial history and integrated catchment erosion rates during latest Pleistocene global cooling.

100

101

102

103

104

105

106

107

108

109

110

111

112

113

114

115

116

117

118

119

120

121

122

123

124

125

126

This research builds on the original Lake Devlin studies, makes use of substantial advances in calibration of the <sup>14</sup>C time scale during the past three decades, and exploits increasing sophistication of other geochronology and imaging techniques that have greatly improved analysis of surficial deposits, events and paleoenvironments. We focus on the following questions: (1) What do the glaciolacustrine sediments suggest about the early formation and persistence of the lake and timing of Pinedale glacial events; (2) what new insights about the Pinedale glaciation do different dating techniques offer, including optically

stimulated luminescence (OSL), a method challenged by deposition from turbid waters; (3) what does new palynological and coleoptera data reveal about latest Pleistocene climate history of this near-treeline area of the Rocky Mountains; and (4) what late Pleistocene glacial and periglacial erosion rate can be inferred from analysis of glacial and paraglacial deposits preserved in the Lake Devlin basin?

133 SETTING

The Lake Devlin catchment allows us to analyze the timing and effects of Pinedale glaciation because of its thick archive of glacial and periglacial sediment, trapped by a long-term, ice-marginal dam. The catchment is cut into the crest of the Front Range on the eastern flank of the Rocky Mountains, USA (Fig. 1) and south of the valley of North Boulder Creek (NBC; Madole, 1986). The range slopes east from elevations over 4000 m down to the Colorado Piedmont and High Plains at 1500 m with correspondingly strong temperature and moisture gradients that control modern altitudinal zonation of vegetation and soil types (Barry, 1973; Birkeland et al., 2003).

Valley glaciers as long as 20 km formed during the Pinedale (Madole, 1976a; Madole et al., 1998; Benson et al. 2005) and flowed from cirques cut into the continental divide at elevations between 3950 and 3650 m. Terminal moraines and trimlines show that glaciers between 180 and 350 m thick (Madole et al., 1998; Ward et al., 2009; Dühnforth and Anderson, 2011) extended down to an elevation of ~2530 m during the Pinedale and 2490 m during the 160 – 130? ka Bull Lake glaciation (Dethier et al., 2003; Madole, 1976b). Modern glaciers are restricted to the uppermost elevations of the Front Range (Benson et al. 2007). Glacial sediment of Pinedale age covers nearly 90% of the formerly glaciated area (Dethier et al., 2003) and extensive periglacial deposits suggest that areas above and adjacent to latest Pleistocene glaciers and at lower elevations experienced permafrost conditions (Völkel et al., 2011).

Three creeks flow through eroded deltas and on fine glaciolacustrine sediment deposited on the former lake bottom (Madole, 1986): Caribou Creek from the southwest, Horseshoe Creek from the west and an unnamed creek that originates in the Rainbow Lakes northwest of Devlin Park (Fig. 1). We refer to the latter drainage as Rainbow Lakes Creek (RLC). Caribou Creek leaves the lake basin through a gap at 2950 m, eroded as waters from Lake Devlin broke through its moraine dam and drained catastrophically into the NBC valley. Crystalline bedrock of Precambrian age, which underlies the lake area, is exposed along the valley margin. However, most of the material around the study site is sediment of Pinedale or Bull Lake age (Gilbert, 1968; Gable, 1969; Gable and Madole, 1976). Madole (1986) summarized the sedimentary and geomorphic evidence for a long-lived ice marginal lake including: (1) well developed wave-cut surfaces; (2) an overflow channel eroded into bedrock; (3) extensive outwash, deltaic and lake-bottom deposits; (4) a prominent Pinedaleaged moraine; and (5) boulder-rich outburst deposits in the NBC valley.

STUDY DESIGN

In this study we employed a broad suite of techniques to explore the chronology, paleoclimate and geomorphology of Pinedale deposits and landforms. Prior to sampling of material for dating, pollen, macrofossil and sediment analysis, we updated previous geologic mapping in the Devlin Park area (Gilbert, 1968; Madole, 1986) in order to locate and relocate key stratigraphic sections on a lidar base (Anderson et al., 2011). We used multiple shallow geophysical techniques (electrical resistivity tomography (ERT), ground-penetrating radar (GPR), and shallow seismic refraction (SSR)) to provide local 3-D control and geologic context for environmental samples. Reconnaissance investigations suggested that fine-grained deltaic sediment might contain pollen and macrofossils useful in paleoclimate analysis, so we sampled two key exposures in detail (Fig. 1). We sampled boulders in moraines and a flood deposit, as well as bedrock surfaces to estimate exposure ages related to deposition and the timing of ice retreat using cosmogenic radionuclides (CRN). Optically stimulated luminescence (OSL) studies provided a context for analyzing the timing of deltaic

growth into Lake Devlin as well eolian deposition that followed drainage of the lake. By combining recalculated published <sup>14</sup>C ages from cores collected previously in Lake Devlin (Madole,1986; 2010) and burial ages from this study we were able to calculate a new age/depth model for lake sedimentation, providing context for pollen, macrofossil and magnetic susceptibility (MS) data (Rosenbaum and Larson, 1983). Synthesizing these data allowed us to reinterpret the ~15,000 yr of geologic events and climate change associated with Lake Devlin's filling, high-stand, and ultimate draining. The combination of field and dating studies and lidar-image analysis allowed us to estimate deposition and erosion rates for the Lake Devlin catchment during and after the Pinedale glaciation.

#### **MATERIAL AND METHODS**

#### **Field Mapping and Geophysical Investigations**

We conducted detailed field mapping of the study area and surveyed 6 transects using geophysical techniques (Fig. 1) and guided by a 1-m lidar hillshade (Anderson et al., 2011) processed by the National Center for Airborne Laser Mapping in August of 2010 as part of the Boulder Creek Critical Zone Observatory studies. The detailed lidar base and geophysical transects (see Supplementary Material--SM) allowed more accurate mapping and precise calculations of areas and volumes of deposits to contribute to our erosion-rate studies.

#### **Sediment Sample Collection**

Sections for textural, stratigraphic, macrofossil and pollen studies were dug by hand from Lake Devlin deltaic and glaciolacustrine deposits (Fig. 1), sediment samples were returned to the lab and dried at 40°C and the <2-mm fraction was separated by sieving for additional analyses. Grain size measurement of the sand fraction used wet sieving and we analyzed the silt and clay fraction using settling tube techniques (Gee and Bauder,1986; Bubel, 2008).

## Sampling and Measurement of Remnant Magnetism and Susceptibility (summarized from Rosenbaum and Larson, 1983)

For paleomagnetic analyses of Lake Devlin cores DP1 and DP2, sample boxes with sharp edges (volume=3.2 cm³) were inserted into half of the core using a center to center spacing of 3 cm, removed, and sealed to prevent sample desiccation. Natural remnant magnetization (NRM) was determined using a spinner magnetometer. Initial measurements demonstrated that disturbing effects of a soft component were largely removed from samples by alternating field (af) demagnetization in relatively low peak fields. All samples were demagnetized at 10 mT; samples from core DP2 also were demagnetized at a field of 15 mT. The low-field MS of each sample was measured using a precisely calibrated, highly sensitive bridge system (Christie and Symons, 1969; Rosenbaum et al., 1979). These data contribute to our understanding of temporal variation in the deposition of fresh magnetic materials in Lake Devlin during the Pinedale.

219 Dating

Forty new samples were submitted and dated by OSL,  $^{14}$ C, and cosmogenic techniques and we used these ages and Madole's (1986; 2010)  $^{14}$ C dates to calibrate a new depth/age model for Lake Devlin deposition and to analyze the sequence of nearby glacial events that drove the formation and disappearance of the glacial lake. We use the following conventions: "ka" for dates in 1000s of years and "kyr" for duration of time in 1000s of years. We report dates from the analysis of 14C, OSL and CRN samples using the following conventions: (1)  $^{14}$ C dates are reported in thousands of years (ka) BP  $\pm$  2 $\sigma$ , in calibrated years (cal BP  $\pm$  2 $\sigma$ ) and as Median Probability age (yr) calculated using Calib Rev. 8.2 (Reimer et al., 2020), consistent with reporting protocols used by the radiocarbon community; (2) OSL ages are reported in ka  $\pm$  1 $\sigma$  with uncertainty calculated from counting statistics (internal error) and (3) Cosmogenic exposure ages are reported in ka  $\pm$  1 $\sigma$  (external error). Geologic uncertainty may be considerably higher, particularly for the cosmogenic exposure ages, as noted below.

237 OSL dating

Twenty samples for luminescence analysis, chosen mainly to date the growth of Lake Devlin deltas, were collected using 20 x 4 cm steel tubes that were hammered into cleaned sediment exposures. Our sampling program was also designed to test whether luminescence analysis would produce stratigraphically and geologically plausible dates in deposits that formed from turbid meltwater. Sampling direction was mostly horizontal. Where the sediments were noncohesive, tubes were hammered vertically to minimize disturbance. Sediment from around each tube was collected for dose rate analysis. Site descriptions included position, elevation, sediment inclination, grain size estimation and other sedimentological parameters.

Under subdued orange light, the outer material of the tubes was discarded and a portion of the inner material processed to extract quartz and K-rich feldspar grains in the 180-250 µm range (Murray et al., 2021, Fig 3a). On another portion the saturated water content was determined using the syringe method (Murray et al., 2021). Only quartz extracted from aeolian material showed suitable luminescence characteristics (e.g., sample 065414 presented in Buylaert et al., 2012). Unfortunately, other samples gave dim quartz signals without a strong fast component, rendering any age determination using quartz from this material unreliable (see SM Fig. 1a,b; Wintle and Murray, 2006; Murray et al., 2021). Equivalent dose measurements were thus carried out on the K-rich feldspar using infra-red stimulated luminescence (IRSL measured at 50°C, IR<sub>50</sub>) and gamma spectrometry was used for dose rate determination (see SM). We chose the IR<sub>50</sub> signal because it is the most readily reset feldspar signal but it is known that this signal also suffers from anomalous fading (Huntley and Lamothe, 2001; Huntley and Lian, 2006) which results in an underestimation of

the age. Here this has been corrected for using laboratory measurements of the fading rate (Huntley and Lamothe, 2001; see also SM Fig. 1c). The radionuclide concentrations and infinite matrix dry beta and gamma dose rates are given in SM Table 1 and calculated luminescence ages in Table 1.

#### Radiocarbon dating

Eleven new samples for radiocarbon dating (seeds from deltaic sections; peat and charcoal from bogs and eolian deposits) were separated from field-sieved material after hand-picking in the laboratory and sent to Beta Analytical for dating by accelerator mass spectrometry. We integrated the new <sup>14</sup>C ages from deltaic sections into a time/depth model for Lake Devlin sediment, extending Madole's (1986) work by converting his 10 dispersed organic carbon dates to calibrated ages, and using newer <sup>14</sup>C ages from the bottom of core DP-2 (Madole, 2010) and the <sup>14</sup>C ages and sample elevations from the RLC delta (Fig. 1 and SM Table 3).

#### Cosmogenic nuclide exposure dating

Nine samples for cosmogenic exposure age analysis were chipped from large, isolated boulders or glacially polished bedrock exposures; we report <sup>10</sup>Be exposure ages for all samples and a <sup>26</sup>Al exposure age for one of the samples (Table 1; see SM). We collected data to help analyze potential topographic shading in the field by measuring the angle to the horizon at 30° intervals from the sample site, ultimately determining that topographic shielding was negligible. We measured average sample thickness in the field and calculated <sup>10</sup>Be and <sup>26</sup>Al exposure ages with Version 3 of the online exposure age calculator formerly known as CRONUS Earth (Balco et al., 2008), using the global production rate dataset, and LSD*n* scaling (see SM Table 6). Samples were prepared at the University of Vermont cosmogenic lab and measured at Lawrence Livermore (CAMS) National Laboratory Calculated ages assume no nuclides inherited from previous exposure and no post-exposure erosion or shielding. Sensitivity analyses demonstrated that choosing different scaling schemes would impact the ages by no more than 8%. Using the Promontory Point

production rate (Lifton et al., 2015) would make ages about 2% younger, well within the limits of external uncertainty (Table 1).

#### **Palynology and Macrofossils**

For samples collected from deltaic and glaciolacustrine exposures for pollen and macrofossil analysis, 20 to 25 kg of sediments were wet-sieved in the field, using a 0.500 mm screen for sandy samples, and clays and silts were washed over a 0.250 mm screen. Material not passing the screens was saved and returned to the laboratory for additional cleaning, drying and analysis as part of our paleoclimate studies. In addition, several samples for pollen analysis were collected along stream exposures or via peat corer in kettle-hole bogs and returned to the laboratory for extraction and analysis. Samples collected for palynological and macrofossil studies were processed in the laboratory for pollen extraction using standard techniques (5% KOH, 10% HCl, 48% HF, and acetolysis for 5 min (Faegri and Iversen, 1975), followed by washing over a 10-µm NITEX screen to remove silt- and clay-sized particles (cf. Cwynar et al., 1979). Pollen residues were mounted in silicone oil and counted at 200X. Macrofossil concentrates that had been pre-screened in the field were dried, dry-sieved into size classes and picked under a microscope in their entirety in the laboratory. Identifications were made based on literature references and the reference collection in the Quaternary Paleoecology Laboratory at Colby College.

#### **Deposit Volumes in the Lake Devlin Basin**

We combined field mapping, geophysical data and GIS-based spatial interpolation methods to estimate volumes of sediment eroded and deposited in the Lake Devlin basin in Pinedale and post-Pinedale time. The upper surface of fine-grained deposits, outlined by field mapping and the base of the deposits, located by borings and by geophysical traverses, defined the irregular wedge of silt and clay that accumulated in Lake Devlin. The difference between the original upper surface of glaciolacustrine deposits and the present landscape provided a minimum estimate for erosion and transport of fine-grained deposits out of the Lake Devlin basin after the lake drained. The original dimensions of the two deltas were

extrapolated from present remnants and thickness defined by geophysical traverses.

Outwash volumes were estimated from deposit thickness beneath outwash terraces.

Calculated volumes for sediment stored in moraines and as till were less-well constrained. Surface areas were measured by lidar analysis. Thicknesses were estimated by the difference between present topography and a model sub-moraine surface calculated from spatial interpolation by inverse distance weighting based on elevations at moraine edges, exposed bedrock, kettle bottoms and stream channels (see SM). This technique gives a maximum volume for Pinedale moraine deposition because moraines may include older material at depth. Erosion in the Horseshoe and Rainbow cirques was estimated by subtracting present topography from a smooth surface interpolated from the cirque margins (see SM).

325 RESULTS

Field, laboratory, and DEM-based studies reported here extend previous work on Lake Devlin and highlight the extensive early Pinedale glacial advance, rapid biotic change at about 15 ka and catastrophic draining of Lake Devlin millennia after ice had retreated upvalley from the lateral moraine that dammed the lake (Dühnforth and Anderson, 2011). Upland erosion recorded by deposition in the Devlin catchment suggests glacial and periglacial erosion rates were about 70 mm kyr<sup>-1</sup> during the Pinedale and that most of the sediment, including half of the glaciolacustrine deposits, remains in the basin.

### **Geological Mapping and Sedimentology**

Geologic mapping of glacial and glaciolacustrine deposits and topographic profiles demonstrate that the Lake Devlin basin and adjacent areas preserve a long record of Pinedale and post-Pinedale deposition and erosion. Extensive Pinedale lateral moraines flank the NBC valley and relatively small moraine complexes and outwash trains are preserved upstream in the valleys tributary to the Lake Devlin basin. The original lake extent

is outlined by a bathtub ring of wavecut, locally depositional surfaces and sharply defined overflow and outburst channels, deltas, and thick lake-bottom deposits (Figs. 1 and 2).

#### Glacial deposits and Lake Devlin landforms and deposits

The Pinedale-age NBC lateral moraine complex that dammed Lake Devlin (Madole, 1986; Duhnforth and Anderson, 2011) consists of short ridges, drainage channels, mounds, and kettle holes (Fig. 2), some filled with organic-rich sediment. Horseshoe and Caribou moraines are less extensive and are flanked by older, boulder-rich deposits that may be of Bull Lake age (Gilbert, 1968; Madole et al.,1998); low moraines and shallow kettles are preserved near Rainbow Lakes. The persistence of Lake Devlin for ~15,000 years

produced well-defined wave-cut surfaces at an average elevation of ~2976 m, bordering a 0.28 km² lake. The wave-cut platform is 2-5 m wide where it truncates bedrock and as wide as 50 m where it cuts into the NBC lateral moraine. In some areas the surface is blanketed by 40 – 60 cm of sandy sediment of aeolian origin. The shallow overflow channel is cut mainly in till and bedrock and extends 1 km to the northeast (Fig. 2; Madole, 1986), terminating in a debris fan that flanks the NBC valley.

358 a a 359 b 360 t 1 361 r 362 r 363 v 364 p

Headward erosion during and after breaching of the moraine cut a channel as much as 33 m deep, eroded ~10<sup>6</sup> m³ of till from the lateral moraine and 3.4 to 4.9 x 10<sup>6</sup> m³ of lake-bottom deposits. Thin glaciofluvial deposits are extensive at the western (Horseshoe) end of the lake, but are not preserved along RLC. Delta remnants are preserved at the western and northern ends of the lake. The Horseshoe delta is relatively small and not well exposed. The northern delta, constructed where RLC flowed into Lake Devlin, exposes an 80 m wide dry valley that divides the delta into two parts and likely formed during lake drainage. The upper part of the delta is well exposed, which allowed us to collect OSL samples that document the timing of delta growth. Deposit texture ranges from boulders embedded in grus at the head of the delta, sandy sediments on the delta slope and distal sandy-silty-clayey deposits. The

delta toe area at 2960 m, referred to as "the bar", exposes interlayered fine glaciolacustrine and sandy delta-slope sediment that is coarser than the nearby lake-bottom sediment sampled by coring at sites DP1 and DP2.

Eroded remnants of Lake Devlin bottom deposits, composed mainly of silty to clayrich sediment, crop out throughout the lower Devlin basin. Silt-rich glaciolacustrine deposits are exposed at elevations as high as ~2975 m near the eastern and western margins of the former lake and at elevations ~2960 beneath colluvial slope deposits along the central and SW margin of the former lake. Most exposures are massive- to thin-bedded, locally laminated clay-rich silt, interlayered with sand-rich deposits near former lake margins (Bubel, 2007). Madole (1986) estimated that the total laminated section of glaciolacustrine sediment he cored originally was about 18 m thick, assuming erosion removed the upper 4 to 5 m of sediment. He counted 1500 laminae in a 3.05 m section of a test core (Madole et al., 1973).

#### **Subsurface Interpretation from Geophysical Surveys**

Geophysical surveys (Fig. 1) highlight subsurface stratigraphy and the local depth to bedrock (Fig. 3). Line ERT-1 extends from the lateral moraine over the RLC delta surface onto the delta toe (Figs. 2 and 3a). The top of the delta consists of reworked morainal material and a zone with high resistivity values of up to 15 k $\Omega$ m, reflecting dry conditions during the survey. Upper delta deposits with high resistivity values (up to 5 k $\Omega$ m) lie above sediment with low resistivity values (< 0.30 k $\Omega$ m) at the base of the delta that correlate with horizontally bedded silt and clay-rich glaciolacustrine sediment. At a depth of ~5 m on the delta slope, as well as on the delta back at ~7 m depth, two zones with thickness of 2 to 4 m (Fig. 3a) and sharply lower electrical resistivity probably reflect more silt-rich, moist sediment deposited when RLC shifted away.

Line ERT-2 (Fig. 3b), collected near the Madole coring site, helps test the lateral continuity of the core data. The upper 2 m are characterized by resistivities between 0.7-1 k $\Omega$ m that overlie 15 m with lower resistivities of 0.02-0.07 k $\Omega$ m. A deeper zone with

slightly higher values (0.07 to 0.20 k $\Omega$ m) underlies the low-resistivity section. The contact at 15 m depth likely reflects the transition from gravelly pre-Pinedale deposits to the initial Lake Devlin glaciolacustrine environment.

In the Horseshoe delta area, Line ERT-3 shows high resistivity (>15 k $\Omega$ m) in the upper 1.7 m of dry glacial outwash, overlying lower resistivities of 0.5 to 1 k $\Omega$ m. At a depth of 6.5 m a second zone of lower resistivity (< 0.18 k $\Omega$ m) corresponds with field mapping of fine sediment that underlies typical deltaic sands and gravels. Line ERT-4 indicates that a thin layer of Holocene stream gravels covers ~10 m of lacustrine fines over ~2 m of coarser sediment. Depth to bedrock is ~12 m.

Line SSR-1 (Fig. 3e), collected at a slightly higher, better drained position near ERT-2, allowed us to determine depth to bedrock. Our three-layer model shows an upper 5–10 m thick low-velocity zone (440 – 520 m s<sup>-1</sup>). The first refractor defines a second zone with velocities of 1542–1690 ms<sup>-1</sup> overlying a second refractor with velocities of 5320 – 6090 m\*s<sup>-1</sup> at depths of >65 m. The upper, low-velocity zone indicates dry and loose deltaic sediments underlain by water saturated sediments with typical p-wave velocities. Layer number 3 has fast p-wave velocities typical of granodioritic bedrock at an elevation of ~2900 m, only 30 – 50 m higher than the bedrock elevation 1.1 km away in NBC. At the western Lake Devlin margin near Horseshoe delta, depth to bedrock is ~12 to 20 m.

Line GPR-1(Fig. 3f) allowed us to measure the deepest and probably oldest parts of bogs in the NBC moraine at an elevation of 2973 m and shows subsurface detail in the peatrich deposits that fill two separate kettle holes 4 to 5 m deep. Basal ages (see Table 1) suggest that organic material began to accumulate in the kettle holes before ~ 11,100 calibrated yr BP.

#### **Dating of Deposits in the Lake Devlin Basin**

We report dates from the analysis of <sup>14</sup>C, OSL and CRN samples (Table 1) from Lake Devlin and adjacent areas, including 10 published previously by Madole (1986; 2010) and renumbered here for continuity. Radiocarbon dating--Table 1 lists 17 radiocarbon dates and information from organic materials. The Calib 8.2 ages are slightly younger than those reported by Madole (2010). Samples R1, R5, R6 and R7, from the organo-mineral sediment contact zone of kettles, provide a minimum limiting age for stabilization of the NBC lateral moraine, and initial revegetation of the nearby landscape before ~10,700 cal. yr BP. Three samples (R9, R12 and R13) are from seeds, moss and other discrete organics in lacustrine sediments beneath or interfingered with deltaic sediments (Fig. 4). We determined median probability ages of ~20.2 ka for the site at Horseshoe Creek and 15.3 ka for the RLC delta, providing maximum <sup>14</sup>C ages for the lake drainage event. Macrofossil material was abundant only in the ~15 ka samples from the RLC delta. Samples R2, R3, R4 and R8 were charcoal pieces within eolian sediments in either kettle holes or sand sheets on the former lake bottom. Two samples yielded modern dates, but R3 gave 4230 cal. yr BP and R8 6380 cal. yr BP.

We calculated a time/depth model (Fig. 5) for Lake Devlin sediment, extending Madole's work by converting his dispersed organic carbon dates to calibrated ages, and using newer <sup>14</sup>C ages from the bottom of core DP-2, and <sup>14</sup>C ages and sample elevations from the two deltas (SM Table 3).

438

439

440

441

442

443

444

418

419

420

421

422

423

424

425

426

427

428

429

430

431

432

433

434

435

436

437

#### Luminescence dating

A total of 20 luminescence ages were measured at a variety of sites, mainly in deltaic sediment (Fig. 2; Table 1), allowing us to establish a chronology of delta construction and extending the radiocarbon-based chronology of Lake Devlin. Samples O6, O7, O10, O13, O16 are representative of the latest period of deposition near the top of the RLC delta. They yielded ages of  $15.4 \pm 1.0$  to  $12.5 \pm 0.7$  ka, consistent with the stratigraphically inverted  $^{14}$ C

ages from the organic material in the lake sediments ( $14.2 \pm 0.2$  to  $15.3 \pm 0.1$  cal yr BP). Basal sedimentation of the RLC delta started before  $22.6 \pm 1.8$  ka (O15) but the chronology is incomplete because we did not sample the older, subsurface deltaic sediment (see Fig. 3a). Samples O11, O14, O17 and O18 represent the exposed middle section of the distal delta and gave ages between  $19.7 \pm 1.4$  and  $14.5 \pm 1.5$  ka. Sediment from the upper Horseshoe delta yielded ages of  $17.6 \pm 3.8$  and  $16.6 \pm 1.6$  ka (O3 and O2). Samples O1, O12, O19 and O20 are eolian sediments deposited after the lake drained. They were dated between  $4.0 \pm 0.2$  ka and  $8.1 \pm 1.1$  ka. It is interesting to note that this provides clear evidence for the complete resetting of the IRSL signal in aeolian sediments (compare  $4.2 \pm 0.1$  cal yr BP for R3 and  $4.3 \pm 0.6$  for OSL sample O1).

445

446

447

448

449

450

451

452

453

454

455

456

457

458

459

460

461

462

463

464

465

466

467

468

469

470

471

Samples O8 and O9 gave anomalous ages of  $12.5 \pm 0.7$  and  $13.9 \pm 0.8$  ka, respectively. The latter two values do not fit the stratigraphic sequence because overlying organic material was dated at ~14.6 –15.3 cal. yr BP (R11a, R13 and R12) and the uppermost sediment gave ages of 15.4 ± 1.0 and 14.6 ± 1.4 ka (O7 and O6). The possible slight underestimation of luminescence ages O8 and O9 compared to the overlying radiocarbon ages (R11a, R12 and R13) makes it unlikely that the IRSL signals in these deltaic sands were insufficiently reset at the time of deposition compared to their subsequent burial period. Although only samples O6 and O8 are considered statistically different (t-test), on average the underlying IRSL ages (O8, O9) are slightly younger than the overlying ages (O6, O7), i.e., they are probably stratigraphically inverted. Differences cannot have arisen because of uncertainties in water content because the lower samples (O8, O9) are already assumed to be saturated and so the dose rate cannot be decreased any further by increasing the water content. The upper samples were assumed to be initially saturated and then, after ~14 ka, to contain a drained water content of 20% of saturation. Even if the water content during the drained period was reduced to zero (very unlikely) the overlying ages would only be reduced by ~1 ka. Thus we do not believe that the possible stratigraphic inversion in the IRSL ages arises from water content assumptions. It is more likely to reflect

minor uncertainties in the degree of resetting at deposition of the upper samples (O6 and O7) or difficulties in measuring and correcting for anomalous fading.

#### Exposure-age dating

Exposure ages derived from boulders and bedrock surfaces provide additional constraints on Pinedale glacial events in the Devlin basin and adjacent areas. Results from three CRN samples are consistent with geologic relations and with other nearby exposure ages and modeling. Concordant <sup>10</sup>Be and <sup>26</sup>Al exposure ages for 99t76 suggest that the Lake Devlin moraine dam stabilized ~ 20 ka, a date comparable to those reported by Duhnforth and Anderson (2011) from the NBC terminal zone. Sample DC0603 indicates that 2 kyr later, at 18 ka, wave erosion exposed the boulder in the middle of the platform eroded into the NBC moraine. Sample DC0604, from a large, imbricated boulder at the surface of the Lake Devlin outburst deposit, provides a minimum-limiting age of ~11.1 ka for the flood, although we note that the calculated exposure age may be too young by 1 to 2 ka because of the deep seasonal snowpack at this protected site (Benson et al., 2004; Schildgen et al., 2005).

Several CRN samples may not provide close constraints on geologic events because their isotopic concentrations suggest processes other than simple exposure. Rounded boulders (samples TCU 3 and 4) from a low-relief landform thought to be a Bull-Lake moraine gave exposure ages of ~35 and 52 ka, respectively, which are younger than the expected age for Bull Lake deposits. Till may have covered the boulders, their surfaces may have eroded following exposure or a combination of the two effects may have yielded apparent exposure ages younger than expected. Samples TCU1 and TCU2 are from bedrock outcrops upvalley from the Lake Devlin moraine dam in an area that Dühnforth and Anderson (2011) show was ice free at ~15 ka. Calculated exposure ages of ~23 ka for both samples suggest inheritance of <sup>10</sup>Be from an earlier period of exposure because the NBC glacier did not erode deeply in this area. Samples TCU5 (21.2 ka) and TCU6 (21.5 ka) are

from a granitic cliff downvalley from the maximum extent of Pinedale ice. The CRN age may reflect exposure after a period of erosion at the LLGM.

# Other Records from Lake Devlin and Bog Deposits Magnetic Susceptibility Data

Magnetic susceptibility (MS) data for cores DPI and DP2 (see Fig. 9 in Rosenbaum and Larson, 1983) display similar patterns. Variation of both records with depth likely reflect basin-wide changes with time in the quantity of magnetite. Low susceptibility of samples from the upper 1.5 m of core DPI, compared to those from the corresponding portion of core DP2, may reflect post depositional iron leaching by deeply rooted plants. With few exceptions, samples from the 5.2-7.5-m depth interval (~20-22.5 ka, Fig. 5) are characterized by relatively high values of MS and relatively low values of anhysteretic remnant magnetization (ARM)/MS. Relatively high values of this ratio are typical of the remainder of the core, indicating that the zone of high MS at ~20 ka has coarser magnetic grain size, which may reflect a lower content of clay-sized particles (Rosenbaum and Larson,1983).

#### Pollen Record and Macrofossils

Pollen diagrams from the Horseshoe Creek and RLC sections are plotted (Fig. 6), along with pollen spectra for three other samples and a modern sample of fine detritus from the floodplain of Caribou Creek, at approximately the center of the Lake Devlin basin.

Though pollen concentrations were below 100 grains cm<sup>-3</sup> in some Lake Devlin samples, less than the 10<sup>3</sup> or 10<sup>4</sup> grains cm<sup>-3</sup> found in many lake sediments (Faegri and Iverson, 1975), some conclusions can be drawn based on samples that provided more robust data.

As Legg and Baker (1980) found, 10-30% of the pollen grains in the Lake Devlin samples were too degraded to be readily identifiable - abraded, crushed, corroded, or some combination thereof. Cretaceous palynomorphs, likely derived from upvalley winds emanating in the plains to the east of the mountains, were also recognized in the upper portion of the Horseshoe Creek section (shaded in Fig. 6), and in one of two samples from

RLC (upper shaded band in Fig. 6). These were coincident with very low Quaternary pollen counts, making it difficult to draw firm paleoenvironmental or climatic conclusions.

The modern spectrum showed a dominance of *Pinus* (pine; 48%) with ~10% each of *Picea* (spruce) and *Artemisia* (sage), 15-20% grass (Poaceae), ~4% greasewood (*Sarcobatus*) and rare grains of other related plants (Chenopodiinae). Arboreal pollen was approximately 60% of the total.

The Pinedale Lake Devlin samples from both the RLC and Horseshoe Creek sections, however, typically contained about 20% arboreal pollen. The pollen record was dominated by *Artemisia* (often 50% of the pollen total) which gradually decreased upwards in the section, suggestive of increasing moisture above the basin. Poaceae was comparable to modern values, but *Sarcobatus* was all but absent while other Chenopodiinae were commonly 3-5% of the pollen total. *Artemisia* increased upwards in Legg and Baker's (1980) diagram from the core of lacustrine sediments stratigraphically lower in the section, suggesting drying of the uplands.

The lower shaded band of the RLC delta section (Fig. 6) likely represents a warming interval at ~ 15 ka, particularly compared to the stratigraphically lower section of Legg and Baker (1980). Higher pine is accompanied by up to 20% spruce pollen concentrations, and the assemblages in this zone also include a variety of more mesic tundra herbs as the more xeric *Artemisia* and grasses decreased. Pine pollen concentrations are lower, but spruce pollen is comparable to or greater than modern values.

The upper shaded band at RLC and the entire shaded band at the Horseshoe Creek delta section (Fig. 6), indicated by elevated pine percentages accompanying increasing arboreal: nonarboreal pollen percentages, may be mainly an artifact of extremely low pollen counts and the dominance of pine and other pollen coming from long-distance transport.

Note that in these shaded bands pollen counts are not only low, but the only ones in either section that show significant contribution of *Betula* (birch) and *Alnus* (alder), and small but significant oak (*Quercus*), all suggesting long-distance transport.

Macrofossil samples generally were too sparse and deficient in diagnostic materials to be able to make definitive environmental conclusions. Fragments of moss, seeds of sedges and aquatic plants, and unidentifiable insect chitin dominated most assemblages and were relatively abundant only in the ~15 to 14 ka deposits adjacent to RLC.

557 558

559

560

561

562

563

564

565

566

567

568

569

570

571

572

573

574

575

576

577

578

579

580

553

554

555

556

#### Rates of Deposition and Erosion

Surface and subsurface evidence shows that Lake Devlin and the Devlin basin served as traps that captured sediment generated by small glaciers in shallow cirques and by periglacial processes on basin slopes, thereby preserving clear evidence of post-Pinedale erosion. This archive allowed us to quantify sediment volumes and to estimate erosion rates during a complete alpine glacial cycle of ~ 15 kyr (Table 2 and SM), assuming steady-state slopes. Erosion during the late and middle (?) Pleistocene excavated ~ 60 m (0.3 km<sup>3</sup>) of bedrock from both the Rainbow and Horseshoe cirques, assuming that local slopes were relatively smooth surfaces when glacial erosion began. Eroded sediment was stored as moraine complexes, talus and till in the upper part of catchment (Fig. 2; Gilbert, 1968) and as outwash, deltaic, and glaciolacustrine deposits in lower areas (Fig. 7). Estimated volume uncertainty is 10 to 30% for the glaciolacustrine and outwash deposits, which are constrained by geologic mapping and geophysical measurements. Uncertainty is greater, perhaps as much as 50% for Pinedale moraine volume, because exposed moraines bury pre-Pinedale deposits at some uncertain depth (Gable and Madole, 1976; Madole et al., 1998). Till, moraines and other coarse deposits in the Devlin basin comprise 5.5 x 10<sup>6</sup> m<sup>3</sup> of debris, some of it pre-Pinedale in age, equivalent to integrated cirque and periglacial erosion rates of 31 to 55 mm kyr<sup>-1</sup>; we did not correct these figures for the ~20% density change between deposits and fractured bedrock. Most moraine sediment remains as legacy deposits.

In the lower Lake Devlin basin, we calculated that  $\sim 2 \times 10^6 \text{ m}^3$  of outwash deposits accumulated beneath terraces along Caribou and Horseshoe Creeks and  $> 6.5 \times 10^6 \text{ m}^3$  of lacustrine sediment nearly filled Lake Devlin over a period of  $\sim 15$  kyr, a larger volume than

that of sediment preserved near the cirques. Total Pinedale deposition in the Lake Devlin catchment is equivalent to an erosion rate of ~ 70 mm kyr<sup>-1</sup>. Moraines, most of the outwash deposits and about 50% of the lacustrine fill remains in the basin, as does a 30 m-thick prism of older sediment beneath the preserved lake deposits (Madole, 1986). Subsurface evidence suggests that the sedimentary fill in the Lake Devlin area is as thick as 60 m, recording substantial local aggradation over pre-glacial topography.

587

589

590

591

592

593

594

595

596

597

598

599

600

601

602

603

604

605

606

581

582

583

584

585

586

588 DISCUSSION

The integrated dating techniques of this study help establish a detailed framework for the Pinedale glaciation and latest Pleistocene events prior to the LLGM, an important period of rapid climate change that is not well documented in the western USA. Glacial Lake Devlin formed in a tributary valley dammed by a glacier that advanced down the NBC valley and persisted for >15 kyr, trapping sediment eroded by small cirgue glaciers and from hillslopes dominated by periglacial processes. Damming at ~30 ka demonstrates that the initial Pinedale advance was nearly as extensive as that of the LLGM and suggests that large early MIS 2 advances may have occurred elsewhere in the western USA (see Rosenbaum et al., 2012; Laabs et al. 2020) where paleoclimate forcing was similar. Glaciolacustrine deposits record cold, dry environmental conditions near treeline in the Front Range during most of the Pinedale glaciation, interrupted by warmer periods after about 15 ka, and by catastrophic drainage before 12 ka. Glacial and periglacial erosion rates during Pinedale time are higher than those measured beyond the glacial limit in the adjacent post-orogenic Front Range, but much lower than those reported from warm-based glaciers flowing on weak rocks in tectonically active zones such as SSE Alaska (Hallet et al., 1996; O'Farrell et al., 2009; Koppes, 2020). These data contribute to ongoing discussions about the amount and significance of glacial erosion to silicate weathering and the global CO<sub>2</sub> cycle.

History of Glacial Lake Devlin and Adjacent Areas

The physical setting and dating of Lake Devlin demonstrate that the early Pinedale NBC glacier must have been nearly as extensive as the LLGM glacier and that blockage by the moraine dam persisted throughout Pinedale time. Exposure-age dating in the adjacent valleys (Ward et al., 2009 and Dühnforth and Anderson, 2011) documented that glaciers retreated from their maximum extents after about 20 ka and into cirque areas before ~14 ka. Pollen, sparse macrofossils, and the MS record in Lake Devlin glaciolacustrine deposits thus extend the record and add paleoclimatic detail for period from ~ 30 ka to 14 ka.

607

608

609

610

611

612

613

614

615

616

617

618

619

620

621

622

623

624

625

626

627

628

629

630

631

632

633

Dating of the sedimentary fill in L. Devin helps extend regional chronologies, which do not document the extent of early Pinedale ice in the Southern Rocky Mountains in detail (Nelson et al., 1979; Young et al., 2011). Fine glaciolacustrine sediment was deposited in glacial Lake Devlin as early as 29.4 ka (Fig. 8), requiring damming by an NBC glacier nearly as extensive as that of the LLGM (Madole, 2010) and deposition continued without a visible break for 15 kyr. Building on the previous <sup>14</sup>C lacustrine chronology of Madole (1986), our research reports the first detailed OSL-record from the Front Range in a glacial-deltaic environment that persisted from before ~23 to ~14 ka (see also Leopold and Dethier, 2007). The oldest luminescence ages, from near the exposed contact of lacustrine sediments and distal deltaic sediments (22.6±1.8 to 19.7±1.4 ka), are some 8 kyr younger than the oldest <sup>14</sup>C age, which is several m deeper and lacustrine. Geophysical evidence shows that the undated basal RLC delta extends below the modern surface (Fig. 3a), but our data do not suggest when flow from RLC first was diverted into the Lake Devlin basin. Water and sediment from RLC might have flowed along the margin of the NBC glacier until it reached its maximum size sometime after 30 ka (Madole, 2010) or the delta may have been more extensive. At the western end of the lake, the Horseshoe delta grew substantially after ~20 ka at the sample site, but we could not sample the deeper, subsurface portions of that delta (see Fig. 3c). The period of rapid growth after ~21 ka at both deltas corresponds with the LLGM in nearby areas. The dated record of deltaic sedimentation stopped by  $13.9 \pm 0.9$  ka. This IRSL age may be slightly younger than the youngest <sup>14</sup>C age of seeds incorporated in

the underlying lacustrine sediments (14.2 cal. kyr BP) and older than the exposure age (11.1±0.7 ka, external uncertainty, sample DC0604) of a single boulder deposited by the Lake Devlin outburst flood. We interpret the exposure age as a minimum because it does not account for snow shielding at the site, which might have represented ~1 to 2 kyr (Benson et al., 2004).

Catastrophic drainage of Lake Devlin probably occurred between 14 and 13 ka and flood debris formed a boulder-rich fan that was deposited in an ice-free NBC valley, covered outwash deposits and is graded to a few meters above the modern stream. Dühnforth and Anderson (2011; Fig. 2) showed that the NBC ice margin had retreated at least 8 km upstream into cirque areas before Lake Devlin drained. Radiocarbon dates from basal organic sediment in kettles in the NBC right lateral moraine provide minimum ages for the deglaciation. Peat started to accumulate at these sites by about 11 ka, suggesting both moraine surface stabilization and warmer climate.

Stratigraphic, MS and palynologic data (Fig. 9) record the long depositional record of Lake Devlin and suggest that a cold, relatively dry climate persisted during most of Pinedale time until sharp oscillations began after ~15 ka. The smoothed MS record includes peaks at about 26 and 16.5 ka, but the most prominent peak at ~20 ka represents the LLGM. Peaks probably indicate increased proportions of relatively coarse, unweathered rock flour (Rosenbaum and Reynolds, 2004; Rosenbaum et al., 2012) in the lacustrine silt. The MS peak at ~20 ka coincides with low AP/NAP values, a trough in the smoothed Picea/Pinus record and CRN dates from the adjacent LBC valley (Dühnforth and Anderson, 2011). Pollen analyses show that after the LLGM and before ~15 ka vegetation was sparse near the lake site; the arboreal – non-arboreal ratio remained low (25-30) and Artemisia concentrations were high (> 50 %), typical of alpine tundra. Legg and Baker (1980) suggested the tree line was at least 100 m below the area of Lake Devlin at 16 ka. After about 15 ka, peaks in the AP/NAP record from the RLC section are higher than any values after 28 ka and correspond with the appearance of alder and birch in the pollen record (Fig. 6) and relatively abundant

macrofossils in the lake sediment. Calculated pollen concentrations are influenced by differences in sedimentation rates at our sample sites, but the record after ~15 ka suggests annual vegetation cover in the basin, growth of a nearby forest and climate that correlates with Bølling-Allerød warming (Briles et al., 2012; Yuan et al., 2013). Peaks are separated by troughs that correspond with high values of Artemisia, suggesting a fluctuating climate that became colder and drier after about 14 ka, before the outburst flood.

After catastrophic drainage of Lake Devlin, rapid headward erosion by fluvial and hillslope processes cut into fine lake-floor deposits and sand-rich deltaic deposits. Local deposition resumed in mid-Holocene time, and sandy eolian deposits accumulated in at least two areas (Fig. 8; Table 1). Environmental conditions must have changed to allow wind erosion and local deposition of sand sheets, in part coeval with maximum rates of eolian silt accumulation in soils formed on Pinedale moraines in nearby catchments (Muhs and Benedict, 2006).

674 Erosion Rates

During Pleistocene cold periods, areas of glacial and periglacial processes expanded globally (Clark et al., 2009), exposing fresh rock surfaces to erosion and potentially increasing weathering rates and contributing to global cooling (Herman et al., 2013). During the cold climates of Pinedale time, erosion of resistant high-grade metamorphic and igneous rocks and regolith in the Lake Devlin catchment occurred at much higher rates than landscape lowering by fluvial and hillslope processes in adjacent, lower-elevation areas of the Front Range. We measured total sediment accumulation rates of ~70 mm kyr<sup>-1</sup> in the partly glaciated Lake Devlin catchment and assume that these rates of deposition are equal to rates of catchment erosion during Pinedale time. The measured rate of sediment accumulation is nearly 3x erosion rate estimates of ~25 mm kyr<sup>-1</sup> (Dethier et al., 2014; Foster and Anderson, 2016) calculated using cosmogenic <sup>10</sup>Be in alluvium from adjacent upland catchments. Sediment deposition rates in the Lake Devlin catchment also exceed the ~40 mm kyr<sup>-1</sup> rates of erosion measured on alpine slopes 8 km north of the study area (Dethier et

al., 2014), but are much less than rates > 1000 mm kyr<sup>-1</sup> reported for warm-based glaciers on erodible rocks (Williams and Koppes, 2019; Koppes, 2020).

Differential rates of erosion by glacial, periglacial and weathering processes are helping to sculpt alpine areas in the Front Range. Small et al. (1997) estimated that unglaciated alpine sites near the crest of the southern Rocky Mountains, low-slope bedrock surfaces are lowering slowly, at rates of 5 to 10 mm kyr<sup>-1</sup>. The Lake Devlin catchment is cutting down and back into the upland at much greater rates, increasing local relief and eroding the crest of the Front Range. Both Devlin basin cirques were excavated into larger catchments where periglacial erosion processes likely dominated during the Pinedale.

Cirque erosion rates must be higher than the overall catchment lowering rate. If we apply the integrated basin rate of 70 mm kyr<sup>-1</sup> and make the improbable assumption that rates have been linear over time, the cirques could have been excavated in <900 kyr.

Most of the sediment eroded from cirques and hillslopes by periglacial and glacial processes during the Pinedale remains in storage in the Lake Devlin catchment. Latest Pleistocene and early Holocene erosion rates were rapid as the channel network became reestablished through easily eroded sediment, but neither channels nor hillslopes appear to be evolving rapidly at present.

#### **Coupling of Climate and Erosion**

This study documents local glacial and periglacial erosion rates of resistant rocks in the Front Range during the cold, relatively dry climates of the latest Pleistocene. Rates are ~3x long-term values measured in catchments beyond the local glacial limit (Dethier et al., 2014). Increased erosion driven by climate change in the post-orogenic landscapes of the Rocky Mountains contributed to continental-scale changes in erosion rates that began in Pliocene time (Zhang et al., 2001). In alpine catchments similar to the Lake Devlin basin, some sediment produced by late Pleistocene erosion may not travel downstream for many millennia or until the next glaciation. Sediment eroded from cirques and hillslopes remains stored in ice-contact deposits such as moraines or trapped in lakes and other zones where

valleys were overdeepened by glacial erosion. However, the fresh mineral surfaces exposed by abrasion and rock cracking likely contribute to increased rates of chemical weathering in the Front Range and in other alpine zones developed in igneous and metamorphic rocks (Anderson et al., 1997). On a global scale, expanded areas of glacial and periglacial processes in areas of silicate-rich rocks may help to buffer atmospheric levels of CO<sub>2</sub> (Herman et al., 2013; Brantley et al., 2023), particularly in cool, moist, orogenic zones such as SE Alaska and the Southern Alps of New Zealand, where sediment production is much greater than those of the southern Rocky Mountains.

723 CONCLUSIONS

The sedimentary record from Lake Devlin adds to the skeletal regional record of substantial early Pinedale advances, which has significant implications for models of latest Pleistocene paleoclimate and contributes to ongoing discussions about the amount and significance of glacial erosion to silicate weathering and the global CO<sub>2</sub> cycle. The early Pinedale NBC glacial advance was extensive, and a suite of dating techniques show that blockage by the moraine dam persisted throughout Pinedale time until Lake Devlin drained catastrophically after the peak of Bølling-Allerød warming, perhaps at about 14 ka. Pollen and macrofossil evidence, combined with the MS record, suggest peaks of glacial activity during the LLGM at ~20.0 ka and at about 26.0 and 16.5 ka, and that local treeline was below Lake Devlin until ~15 ka. Glacial and periglacial erosion rates averaged ~70 mm kyr<sup>-1</sup> during Pinedale time, exposing fresh surfaces and sediment, but most of the sediment remains in the Lake Devlin catchment as glacial and glaciolacustrine deposits.

#### **ACKNOWLEDGMENTS**

We are grateful for the data and logistical help provided by the NSF-sponsored NWT Long Term Ecological Research (LTER) project and the University of Colorado Mountain Research Station. Logistical support and/or data were provided by the German Research Foundation (DFG) who supported the field work and analysis via two grants (DFG LE1531-1

- and LE1531-2), and the Boulder Creek Critical Zone Observatory (NSF 0724960) and NSFEAR 1735676 helped support the cosmogenic radionuclide studies. We also thank Craig
  Skeie, at the time Water Resources Facility Manager, City of Boulder watershed, for his help
  with access and logistics in Devlin Park. The Keck Geology Consortium (NSF 1062720)
- supported students who helped in the data acquisition. We further greatly thank Dr. Juliane
- Huber from the Technical University of Munich, Germany, for her work and discussions over
- a time span of more than 10 years.

749 750

#### REFERENCES CITED

- Anderson, Suzanne Prestrud, Drever, James I., and Humphrey, Neil F., 1997, Chemical weathering in glacial environments: Geology, v. 25(5), p. 399-402.
- Anderson, S. P., Guo, Q., and Parrish, E., 2011, *Snow-Off Digital Terrain Model (DTM) from* 2010 LiDAR for the Boulder Creek Critical Zone Observatory (CZO),
- 755 Colorado: Environmental Data Initiative.
- 756 <u>https://doi.org/10.6073/pasta/458c3932f7786b1da02a9c900baf594b</u>. Dataset accessed 6/11/2019.
- Balco, G., Stone, J.O., Lifton, N.A., Dunai, T.J., 2008, A complete and easily accessible
   means of calculating surface exposure ages or erosion rates from 10Be and 26Al
   measurements: Quat. Geochronol. https://doi.org/10.1016/j.quageo.2007.12.001
- Barry, R.G., 1973, A climatological transect on the east slope of the Front Range, Colorado: *Arctic and Alpine Research* 5, 89-110.
- Benson, L., Madole, R., Phillips, W., Landis, G., Thomas, T., Kubik, P., 2004, The probable
   importance of snow and sediment shielding on cosmogenic ages on north-central
   Colorado Pinedale and pre-Pinedale moraines: Quaternary Science Reviews 23, 193–
- 766 206.
- Benson, L., Madole, R., Landis, G., & Gosse, J., 2005, New data for late Pleistocene Pinedale alpine glaciation from southwestern Colorado: *Quaternary Science Reviews* **24**(1–2), 49–65.
- Benson, L., Madole, R. Kubik, P. & McDonald, R., 2007, Surface-exposure ages of Front
  Range moraines that may have formed during the Younger Dryas, 8.2 cal ka, and Little
  Ice Age events: *Quaternary Science Reviews* **26**: 1638–1649.
- Birkeland, P.W., Shroba, R.R., Burns, S.F., Price, A.B. & Tonkin, P.J., 2003, Integrating soils and geomorphology in mountains – an example from the Front Range of Colorado: Geomorphology **55**: 329-344.
- Blaauw, M., Christen, J.A., 2011, Flexible paleoclimate age-depth models using an autoregressive gamma process: Bayesian Analysis 6, 457–474.

- Blackwelder, E., 1915, Post-Cretaceous history of the mountains of central western Wyoming: J. Geol. 23, 97-117, 193-217, 307-340.
- Brantley, S.L., Shaughnessy, Andrew, Lebedeva, Marina I., and Balashov, Victor N., 2023, How temperature-dependent silicate weathering acts as Earth's geological thermostat: Science, v. 379, p. 382-389.
- Briles, C.E., Whitlock, C., Meltzer, D.J., 2012, Last glacial-interglacial environments in the southern Rocky Mountains, USA and implications for Younger Dryas-age human occupation: Quat. Res. 77, 96e103. <a href="http://dx.doi.org/10.1016/yqres2011.10.002">http://dx.doi.org/10.1016/yqres2011.10.002</a>.
- Bubel, A. J., 2008, Geomorphology of Devlin's Park and the Caribou Creek catchment
   Colorado Front Range: [Undergraduate thesis]. [Williamstown (MA)], Williams College.
- Buylaert J.-P., Jain, M., Murray, A.S., Thomsen, K.J., Thiel, C., and Sohbati, R., 2012, A robust feldspar luminescence dating method for Middle and Late Pleistocene sediments:

  Boreas, 41 (3), pp. 435 451.
- Clark, P.U., Dyke, A.S., Sakun, J.D., Carlson, A.E., Clark, J., Wohlfarth, B., Mitrovica, J.X., Hostetler, S.W., McCabe, A.M., 2009, The Last Glacial Maximum: Science: Vol. 325, Issue 5941, pp. 710-714 DOI: 10.1126/science.1172873
- 794 Christie, Kyle and Symons, David T. A.,1969, Apparatus for measuring magnetic 795 susceptibility and anisotropy: Geol. Surv. Can., Pap., 69-41, 10 pp.
- Cwynar, L. C., Burden, E., and McAndrews, J. H., 1979, An inexpensive sieving method for concentrating pollen and spores from fine-grained sediments: *Canadian Journal of Earth Sciences*, 16: 1115-1120.
- Davis, P.T., Menounos, B., Osborn, G., 2009, Holocene and latest Pleistocene alpine glacier fluctuations: a global perspective: Quaternary Science Reviews 28, 2021–2033.
- Dethier, D.P., Birkland, P.W. and Shroba, R.R., 2003, Quaternary stratigraphy, geomorphology, soils and alpine archaeology in an alpine to plains transect, Colorado Front Ranges. – Easterbrook, D.J. (ed.): Quaternary Geology of the United States, INQUA 2003 field guide volume, Desert Research Institute, Reno, NV 81-104.
- Dethier, D.P., Ouimet, William B., Bierman, Paul R., Rood, Dylan H., and Balco, Greg, 2014, Basins and bedrock: Spatial variation in <sup>10</sup>Be erosion rates and increasing relief in the southern Rocky Mountains, USA: Geology, v. 42; no. 2; p. 167–170; Data Repository item 2014044.
- Dühnforth, Miriam, and Robert S. Anderson, 2011, Reconstructing the Glacial History of Green Lakes Valley, North Boulder Creek, Colorado Front Range: *Arctic, Antarctic, and Alpine* Research, vol. 43, no. 4, p. 527–542.
- Faegri, K. and Iversen, J., 1975, *Textbook of Pollen Analysis:* New York: Hafner Press. 295 pp.
- Foster, Melissa and Anderson, Robert S., 2016, Assessing the effect of a major storm on 10Be concentrations and inferred basin-averaged denudation rates: Quaternary Geochronology, 34: 58-68. DOI: 10.1016/j.quageo.2016.03.006
- Gable, D. J.,1969, Geological Map of the Nederland Quadrangle, Boulder and Gilpin Counties, Colorado: U.S. Geological Survey Geologic Quadrangle Map GQ-833, scale 1:24,000.

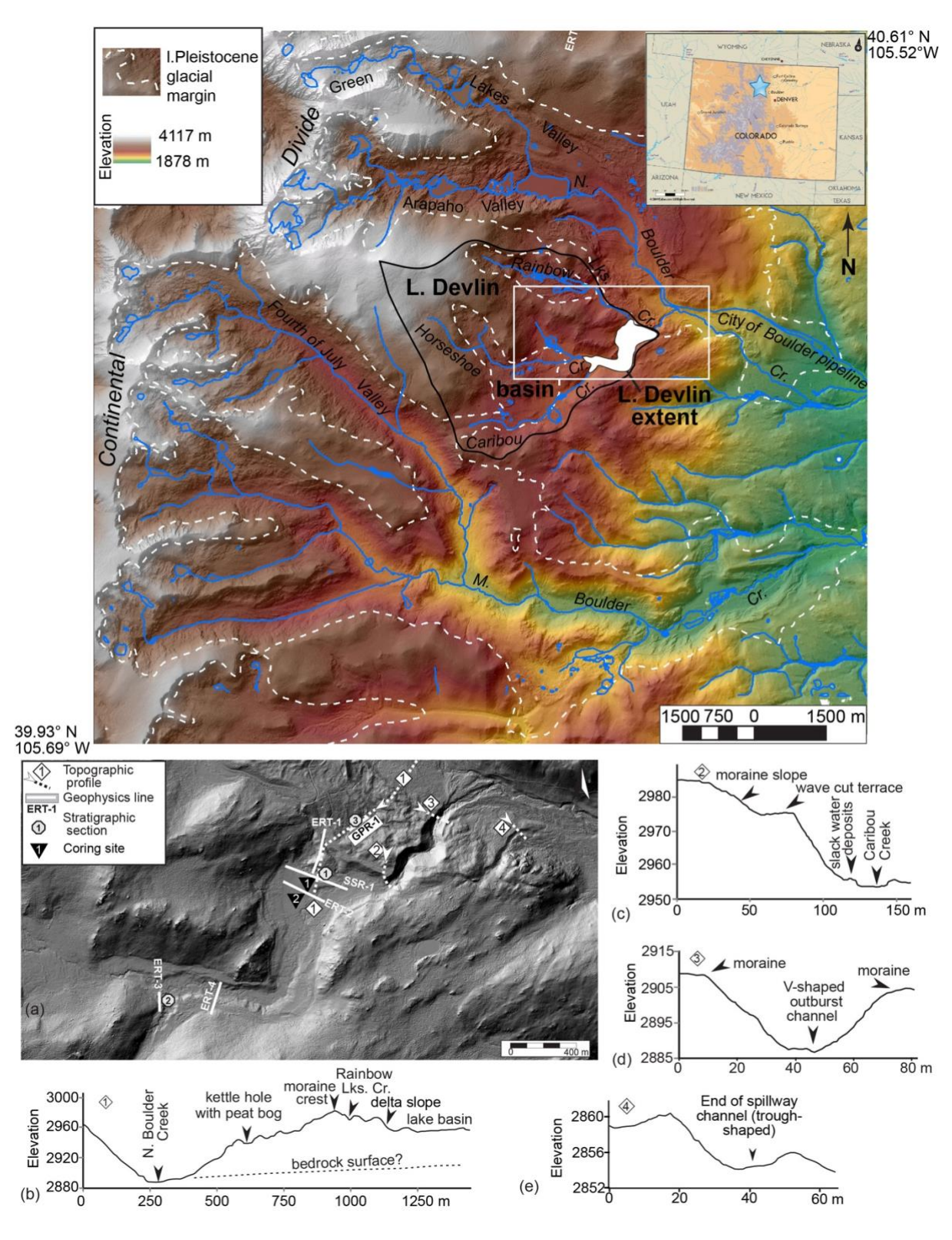
- Gable, D. J., and Madole, R. F.,1976, Geologic map of the Ward quadrangle, Boulder County,
   Colorado: U.S. Geological Survey Geologic Quadrangle Map GQ-1277, scale 1: 24.000.
- Gee, G.W., Bauder, J.W., 1986, Particle-size analysis, In: Klute, A. (Ed.), Methods of Soil
- Analysis, Part 1. Physical and Mineralogical Methods, Second ed.: Agronomy
- Monograph No. 9. American Society of Agronomy/Soil Science Society of America,
- 825 Madison, WI, pp. 383–411.
- Gilbert J. R., 1968, Late Pleistocene history of Caribou Creek valley, Boulder County,
- 827 Colorado: Boulder, University of Colorado M.S. thesis, 53 p.
- Hallet, B., Hunter, L. and Bogen, J., 1996, Rates of erosion and sediment evacuation by
- glaciers: a review of field data and their implications: Global Planet. Change 12, 213–
- 830 235.
- Herman, F., Seward, D., Valla, P.G., Carter, A., Kohn, B., Willett, S.D. and Ehlers, T.A.,
- 2013. Worldwide acceleration of mountain erosion under a cooling climate: Nature, 504,
- 833 423–426.
- Huntley, D.J., Lian, O.B., 2006, Some observations on tunnelling of trapped electrons in
- feldspars and their implications for optical dating. Quaternary Science Reviews 25,
- 836 2503-2512.
- Koppes, Michele, 2020, Rates and Processes of Glacial Erosion: 10.1016/B978-0-12-
- 838 818234-5.00032-8.
- 839 Laabs, B.J.C., Licciardi, J.M., Leonard, E.L., Munroe, J.S., and Marchetti, D.W., 2020, A
- review of updated cosmogenic chronologies of Pleistocene moraines in the western
- U.S. and associated paleoclimatic inferences: Quaternary Science Reviews
- 842 242:106427-106427.
- Legg, T. and Baker, R.,1980, Palynology of Pinedale sediments, Devlins Park, Boulder
- County: Arctic and Alpine Research, 12/3: 319-333.
- Leopold, M., and Dethier, D., 2007, Near surface geophysics and sediment analysis to
- precisely date the outbreak of glacial Lake Devlin, Front Range Colorado, USA: Eos
- Trans. AGU, 88(52), Fall Meet. Suppl., Abstract H51E-0809.
- Lifton, N., Caffee, M., Finkel, R., Marrero, S., Nishiizumi, K., Phillips, F.M., Goehring, B., et
- al.., 2015, In situ cosmogenic nuclide production rate calibration for the CRONUS Earth
- project from Lake Bonneville, Utah, shoreline features: Quaternary Geochronology 26,
- 851 56–69.
- Madole, R. F., Bachhuber, F. W., and Larson, E. E., 1973, Geomorphology, Palynology, and
- Paleomagnetic Record of Glacial Lake Devlin, Front Range: Geological Society of
- America, Rocky Mountain Section 26th Annual Meeting, Guidebook (Trip 1).
- Madole, R.F., 1976a, Glacial geology of the Front Range, Colorado. Mahaney, W. (Ed.):
- Quaternary Stratigraphy of North America: Dowden, Hutchinson and Ross,
- 857 Pennsylvania: 297-318.
- Madole, R.F., 1976b, Bog stratigraphy, radiocarbon dates and Pinedale to Holocene glacial
- history in the Front Range of Colorado: Journal of Research of the US Geological Survey,
- 860 4: 163-169.

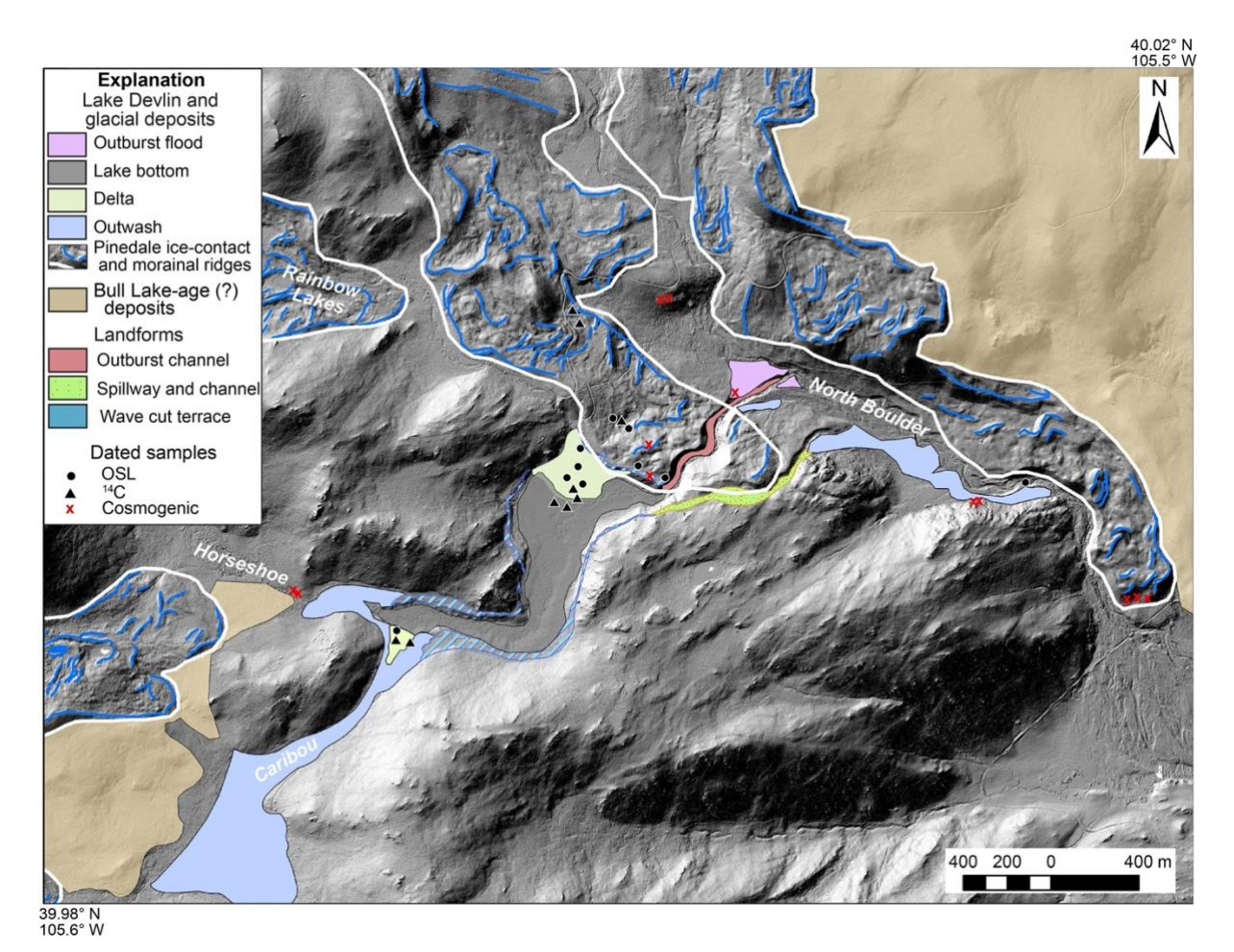
- Madole R.F., 1986, Lake Devlin and Pinedale glacial history, Front Range, Colorado:
- Quaternary Research 25: 43–54.
- Madole, R.F., VanSistine, D.P., and Michael, J.A., 1998, Pleistocene Glaciation in the Upper
- Platte River Drainage Basin Colorado: U S. Geological Survey Investigations Series I-
- 865 2644.
- Madole, R. F., 2010, Evidence from the Front Range, Colorado, indicates that Pinedale
- glaciation began before 31,000 yr ago.: Geological Society of America Abstracts with
- 868 Programs, 42: 363.
- Mahan, S.A., Gray, H.J., Pigati, J.S., Wilson, J., Lifton, N.A., Paces, J.B., Blaauw, M., 2014,
- A geochronologic framework for the Ziegler Reservoir fossil site, Snowmass Village,
- 871 Colorado: Quaternary Research 82, 490–503.
- 872 Muhs, Daniel R. and Benedict, J. B., 2006, Eolian additions to late Quaternary alpine soils,
- 873 Indian Peaks Wilderness Area, Colorado Front Range: Arctic, Antarctic, and Alpine
- 874 Research, 38: 120-130.
- 875 Murray, A.S, Arnold, L.J, Buylaert, J-P, Guerin, G., Qin, J., Singhvi, A.K., Smedley, R., and
- Thomsen, K.J., 2021, Optically stimulated luminescence dating using quartz, 1:72, 1-
- 31: Nature Reviews Methods Primers 1, 72. https://doi.org/10.1038/s43586-021-
- 878 00068-5.
- Nelson, A.R., Millington, A.C., Andrews, J.T., Nichols, H., 1979, Radiocarbon-dated upper
- Pleistocene glacial sequence, Fraser Valley, Colorado Front Range: Geology 7, 410–
- 881 414.
- O'Farrell, Colin R., Heimsath, Arjun M., Lawson, Daniel E., Jorgensen, Laura M., Evenson,
- Edward B., Larson, Grahame, and Denner, Jon, 2009, Quantifying periglacial erosion:
- insights on a glacial sediment budget, Matanuska Glacier, Alaska: Earth Surf. Process.
- 885 Landforms 34, DOI: 10.1002/esp.1885.
- Phillips, F.M., Zreda, M.G., Benson, L.V., Plummer, M.A., Elmore, D., Sharma, P., 1996,
- Chronology for fluctuations in late Pleistocene Sierra Nevada glaciers and lakes:
- 888 Science 274 (5288), 749-751.
- Pierce, K.L., Obradovich, J.D., Friedman, I., 1976, Obsidian hydration dating and correlation
- of Bull Lake and Pinedale glaciations near West Yellowstone, Montana: Geol. Soc. Am.
- 891 Bull. 87, 703-710.
- 892 Quirk, Brendon J., Huss, Elizabeth, Laabs, Benjamin J. C., Leonard, Eric, Licciardi, Joseph,
- 893 Plummer, Mitchell A., and Caffee, Marc W., 2022, Late Pleistocene glacial chronologies
- and paleoclimate in the northern Rocky Mountains: Clim. Past, 18, 293–312,
- 895 https://doi.org/10.5194/cp-18-293-2022.
- Reimer P, Austin WEN, Bard E, Bayliss A, Blackwell PG, Bronk, Ramsey C, Butzin M.,
- 897 Edwards RL, Friedrich M, Grootes PM, Guilderson TP, Hajdas I, Heaton TJ, Hogg A,
- Kromer B, Manning SW, Muscheler R, Palmer JG, Pearson C, van der Plicht J, Reim,
- Richards DA, Scott EM, Southon JR, Turney CSM, Wacker L, Adolphi F, Büntgen U,
- 900 Fahrni S, Fogtmann-Schulz A, Friedrich R, Köhler P, Kudsk S, Miyake F, Olsen J.,
- 901 Sakamoto M, Sookdeo A, Talamo S., 2020, The IntCal20 Northern Hemisphere

- radiocarbon age calibration curve (0-55 cal kB): Radiocarbon 62.
- 903 doi:10.1017/RDC.2020.41.
- 904 Rosenbaum, J.G., Reynolds, R.L., 2004, Record of Late Pleistocene glaciation and
- deglaciation in the southern Cascade Range: II. Flux of glacial flour in a sediment core
- 906 from Upper Klamath Lake, Oregon: Journal of Paleolimnology 31, 235–252.
- Rosenbaum, J., E. Larson, R. Hoblitt, and F. R. Fickett, 1979, A convenient standard for low-field susceptibility calibration: Rev. Sci. Instrum.,50, 1027-1029.
- Rosenbaum, J.G., Reynolds, R. L. and Colman, Steven M., 2012, Fingerprinting of glacial silt in lake sediments yields continuous records of alpine glaciation (35–15ka), western
- 911 USA: Quaternary Research, v.78, p. 333-340.
- 912 Rosenbaum, J. G. and Larson, E. E., 1983, Paleomagnetism of two late Pleistocene lake
- basins in Colorado: An evaluation of detrital remanent magnetization as a recorder of
- the geomagnetic field: Jour. Geophys. Res., v. 88 (B12), p.10611-10624.
- 915 Schildgen, T.F., Phillips, W.M., and Purves, R.S., 2005, Simulation of snow shielding
- orrections for cosmogenic nuclide surface exposure studies: Geomorphology 64 (2005)
- 917 67–85.
- 918 Small, E.E., Anderson, R.S., Repka, J.R., and Finkel, R., 1997, Erosion rates of alpine
- bedrock summit surfaces deduced from in situ 10Be and 26Al: Earth and Planetary
- 920 Science Letters, v. 150, p. 413–425, doi:10.1016/S0012-821X (97)00092-7.
- 921 Schweinsberg, A.D., Briner, J.P., Licciardi, J.M., Shroba, R.R., and Leonard, E.M., 2020,
- Osmogenic 10Be exposure dating of Bull Lake and Pinedale moraine sequences in the
- Upper Arkansas valley, Colorado Rocky Mountains, U.S.A: Quaternary Research. DOI:
- 924 10.1017/qua.2020.21.
- Völkel, J., Huber, J., Leopold, M, 2011, Significance of slope sediments layering on physical
- 926 characteristics and interflow within the Critical Zone Examples from the Colorado
- 927 Front Range, USA: Applied Geochemistry 26 (2011) S143–S145.
- 928 <u>https://doi.org/10.1016/j.apgeochem.2011.03.052</u>
- 929 Walczak, M.H., Mix, A.C., Cowan, E.A., Fallon, S., Fifield, L.K., Alder, J.R., Du, J., Haley, B.,
- Hobern, T., Padman, J., Praetorius, S.K., Schmittner, A., Stoner, J.S., Zellers, S.D.,
- 2020, Phasing of millennial-scale climate variability in the Pacific and Atlantic Oceans:
- 932 Science. 370(6517):716-720. doi: 10.1126/science.aba 7096.
- Ward, D. J., Anderson, R. S. Guido, Z. S., and Briner, J. P., 2009, Numerical modeling of
- osmogenic deglaciation records, Front Range and San Juan mountains, Colorado: J.
- 935 Geophys. Res., 114, F01026, doi:10.1029/2008JF001057.
- 936 Williams, H.B. and Koppes, M. N., 2019, A comparison of glacial and paraglacial denudation
- responses to rapid glacial retreat: Annals of Glaciology 60(80), 151–164.
- 938 <u>https://doi.org/10.1017/aog.2020.1</u>
- 939 Young, N.E., Briner, J.P., Leonard, E.M., Licciardi, J.M., Lee, K., 2011, Assessing climatic
- and non-climatic forcing of Pinedale glaciation and deglaciation in the western United
- 941 States: Geology 39, 171e174. <a href="http://dx.doi.org/10.1130/G31527.1">http://dx.doi.org/10.1130/G31527.1</a>.

942 943 944 945	change in the southern Rocky Mountains from sediments in San Luis Lake, Colorado, USA: Palaeogeogr. Palaeoclim. Palaeoecol. 392, 146-160. <a href="http://dx.doi.org/10.1016/j.paleo2013.09.016">http://dx.doi.org/10.1016/j.paleo2013.09.016</a> .
946 947 948 949	Zhang, Hongbin, Griffiths, Michael L., Chiang, John C. H., Kong, Wenwen, Wu, Shitou, Atwood, Alyssa, Huang, Junhua, Cheng, Hai, Ning, Youfeng, and Xie, Shucheng, 2018, East Asian hydroclimate modulated by the position of the westerlies during Termination I: Science 362, 580–583.
950 951 952	Zhang, P., Molnar, P. and Downs, W. R., 2001, Increased sedimentation rates and grain sizes 2–4 Myr ago due to the influence of climate change on erosion rates: Nature 410: 891–897.
)53 )54	
955	
956	LIST OF FIGURES AND TABLES
957	
958 959 960 961 962 963 964 965 966 967	Figure 1. Map showing the Lake Devlin area and extent of late Pleistocene glaciers (Madole et al.,1998). (a) Inset map showing location of profiles, geophysical lines, coring sites (Madole, 1986) and stratigraphic sections plotted on a lidar hillshade map of the Lake Devlin area. (b) Profile 1 extends from above N. Boulder Creek SW across the valley and Pinedale glacial deposits with kettle holes and lateral moraine ridges towards the moraine crest that dammed Lake Devlin, terminating at the eroded toe of the delta built by Rainbow Lakes Creek (RLC) into Lake Devlin. Bedrock surface inferred from shallow seismic refraction. (c) Profile 2 curves S. from the moraine slope across the nearly flat wave-cut terrace down to Caribou Creek and then SE across Caribou Creek to the wave-cut surface. d) Profile 3 extends across the channel eroded by the Lake Devlin outburst flood. (e) Profile 4 extends across the overflow channel, cut mainly in bedrock and till.
969 970 971 972 973	Figure 2. Glacial deposits and landforms of the glacial Lake Devlin area (modified from Gilbert, 1968) and location of samples collected for dating, plotted on a hillshade map based on bare earth 1-m lidar data (Anderson et al., 2011). Deposits in the NE map area are of pre-Pinedale age. Easternmost cosmogenic sample sites at moraine edge are from Dühnforth and Anderson (2011).
974 975 976 977	Figure 3. Annotated ERT surveys (a-d) and a SSR survey (e) of the Lake Devlin area, and a GPR survey (f) of the cored peat bog area, showing calibrated <sup>14</sup> C ages. Line locations shown on Fig. 1. Note different horizontal scales, line orientations and resistivity color scales. (See SM for detailed caption).
978 979 980 981	Figure 4. Stratigraphic sections from the distal Rainbow Lakes Creek delta and the Horseshoe delta (see Fig. 2) showing the location of dated material and pollen samples. <sup>14</sup> C dates are median probability, in kyr (see Table 1). Inset images a, b, and c show macrofossil material extracted from large (>15 kg) samples of lacustrine clavey silt.

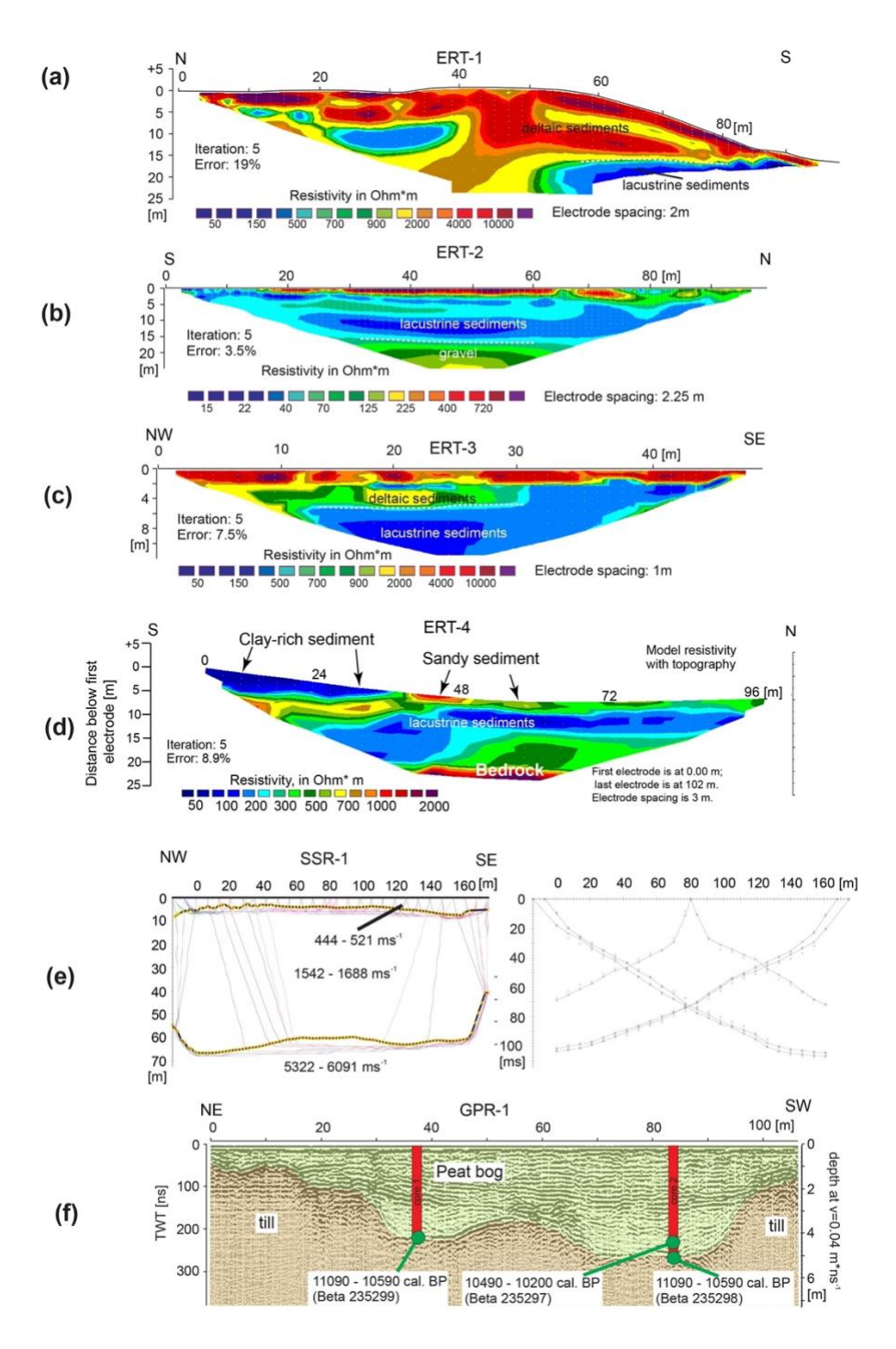
- 982 Figure 5. Bacon age-depth model (Bayesian accumulation histories for deposits; Blaauw and Christen, 2011) using 14C ages from the Lake Devlin DP2 core and adjacent RLC 983 984 section, which extended ~1.6 m above the top of the core (Table 1; SM Table 3). Upper panels (left to right) represent the number of Markov Chain Monte Carlo (MCMC) 985 iterations used to generate gray-scale graphs, prior (green) and posterior (gray) 986 distributions of sediment accumulation rates, and prior (green) and posterior (gray) 987 988 distributions of memory. Main panel shows posterior age-depth results of Bacon modeling (gray) and individual <sup>14</sup>C ages (blue). Gray dots indicate the model's 95% 989 probability intervals. We prescribed prior settings for accumulation rates using a gamma 990 distribution (shape 1.5) and a mean of 10 yr/cm and controlled variations in the 991 accumulation rate between adjacent depths (memory) using a Beta distribution and 992 993 default values: strength of 4 and a mean value of 0.7 (model description modified from 994 Mahan et al., 2014).
- 995 Figure 6. Plots for modern pollen and for pollen from late Pleistocene stratigraphic sections in the Lake Devlin basin (see Fig. 4). (a) Modern pollen distribution sample for organic 996 997 sediment beside Caribou Creek (green shading) and 3 samples of Lake Devlin bottom 998 deposits. Note the high arboreal/non-arboreal pollen ratio and the low percentages of 999 Artemisia in the modern sample compared to those in the Lake Devlin deposits. (b) Pollen 1000 concentration diagram for samples from the RLC delta. (c) Pollen concentration diagram 1001 for samples from the Horseshoe Creek delta. Yellow shading in both (b) and (c) highlights 1002 zones where pollen assemblages suggest warming temperatures. For more elaboration, 1003 however, see text.
- Figure 7. Estimated sediment volumes in the Lake Devlin basin. Values are for Pinedale or post-Pinedale time except for cirque volumes, which may represent erosion over middle and late Pleistocene time.
- Figure 8. Schematic cross section showing landforms, sedimentary units, and selected ages (OSL, <sup>14</sup>C and cosmogenic exposure) from the NBC area and the glacial Lake Devlin basin. Contact locations are based on geophysical and geomorphic results from this study and Madole (1986); dates are from Table 1. Not all dated sites were in the vicinity of the cross section. Sample O18 (16.2 ± 1.0 ka) projects in the same location as O17 and is not plotted. RLC delta bedding dips from 10 to 25°. Note the gap in the cross section between the main lake basin and the Horseshoe delta area.
- 1014 Figure 9. Summary diagram showing integrated stratigraphic information and pollen data 1015 from the Lake Devlin core and adjacent Rainbow Lakes Creek (RLC) section, and smoothed plots (weighted curve fits use the locally weighted least squares error (Lowess) 1016 1017 method with 0.4 smoothing parameter) from the core summarizing the arboreal/nonarboreal pollen percentage (replotted from Legg and Baker, 1980) and MS 1018 1019 (core DP-2, replotted from Rosenbaum and Larson, 1983). Blue and light orange shading 1020 highlight the LLGM and inferred Bølling-Allerød interval, respectively, in the Lake Devlin 1021 basin.

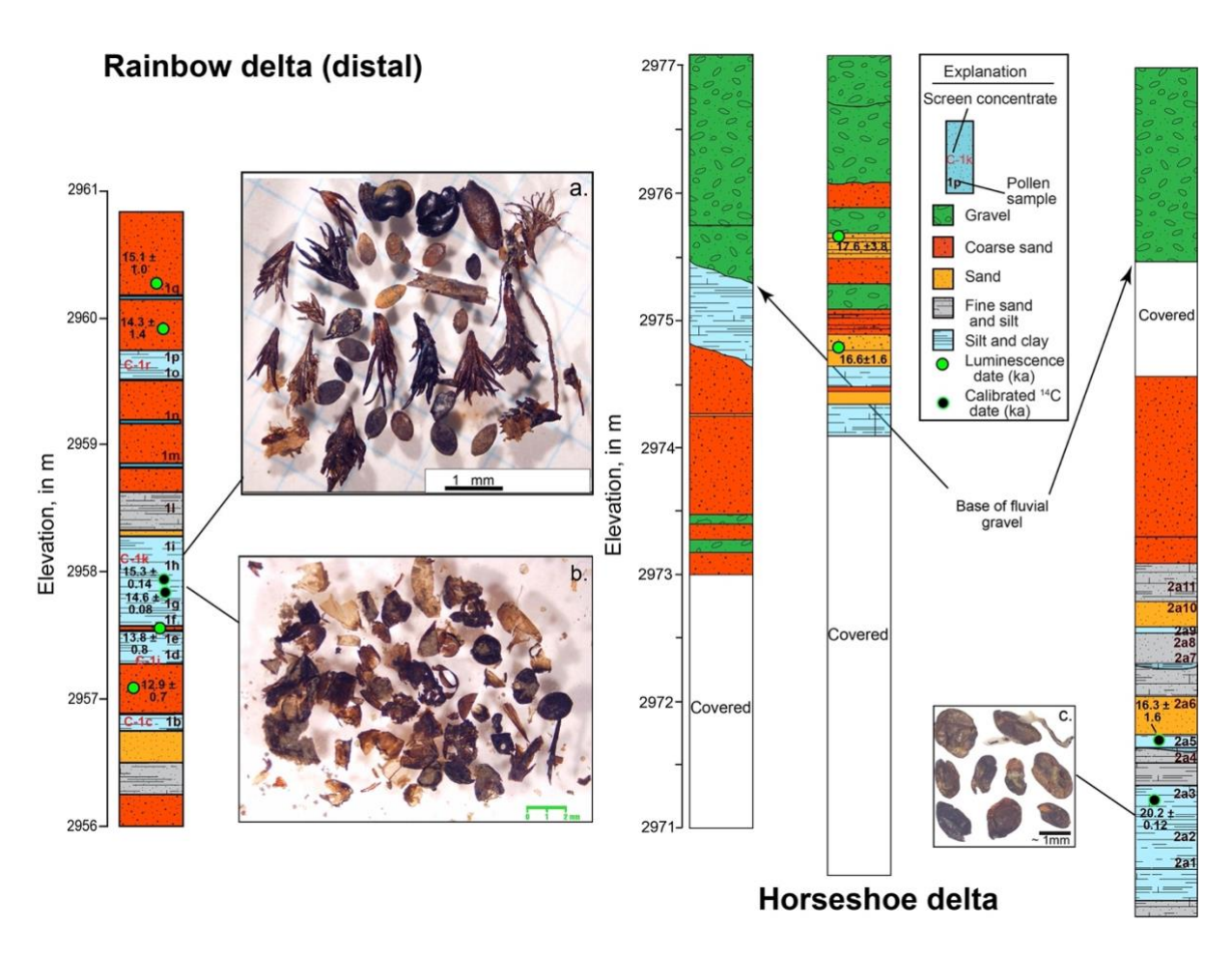


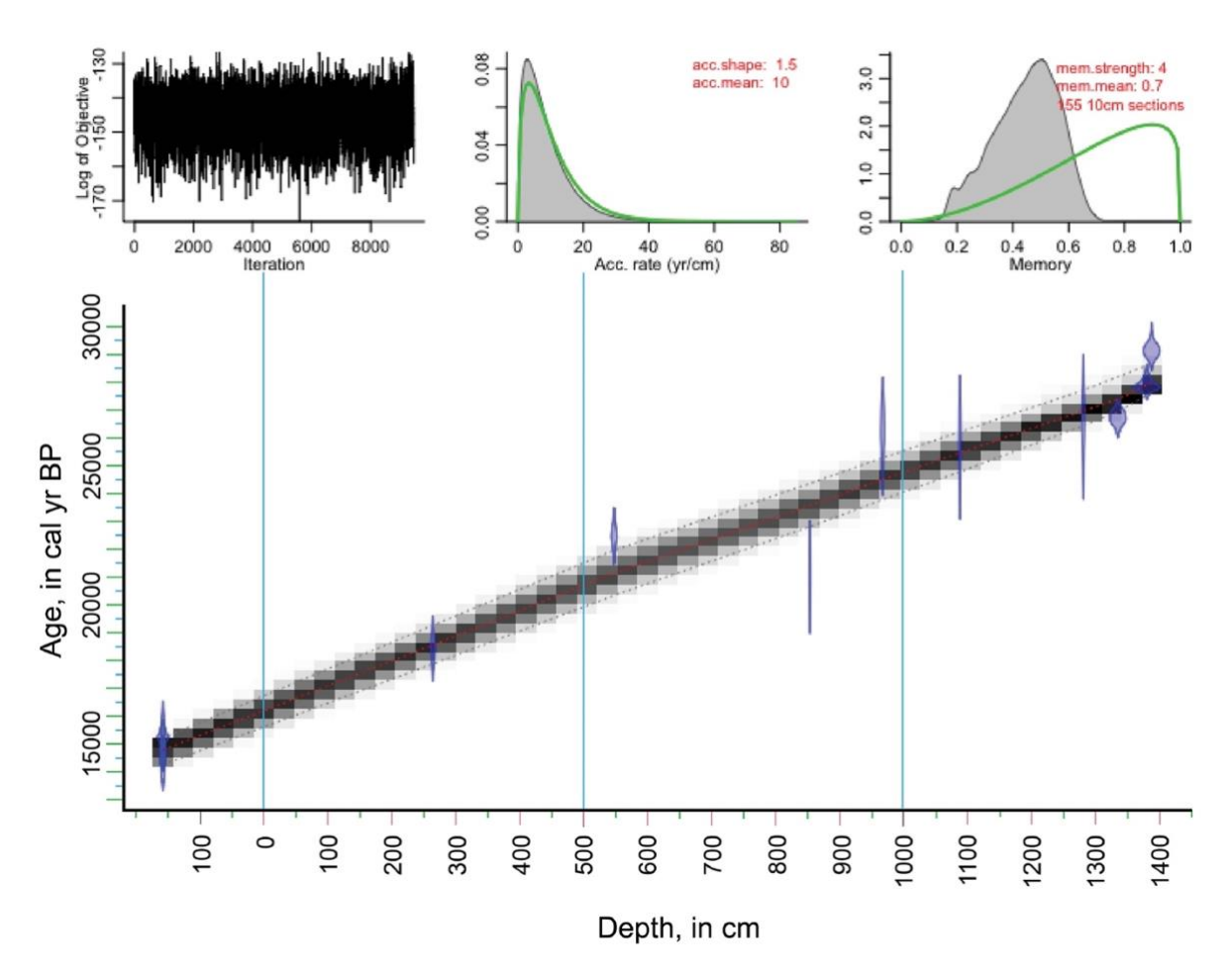


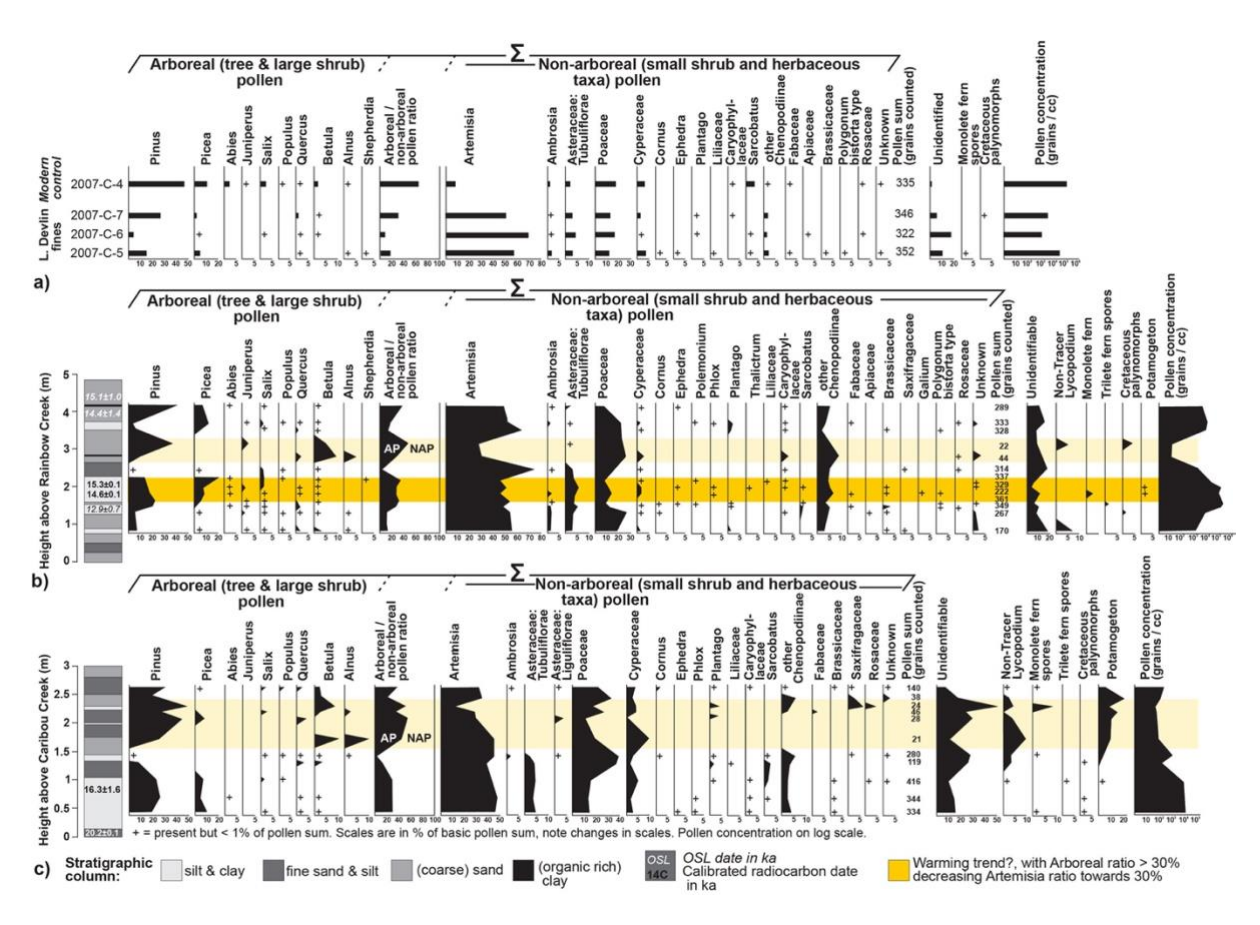
1024

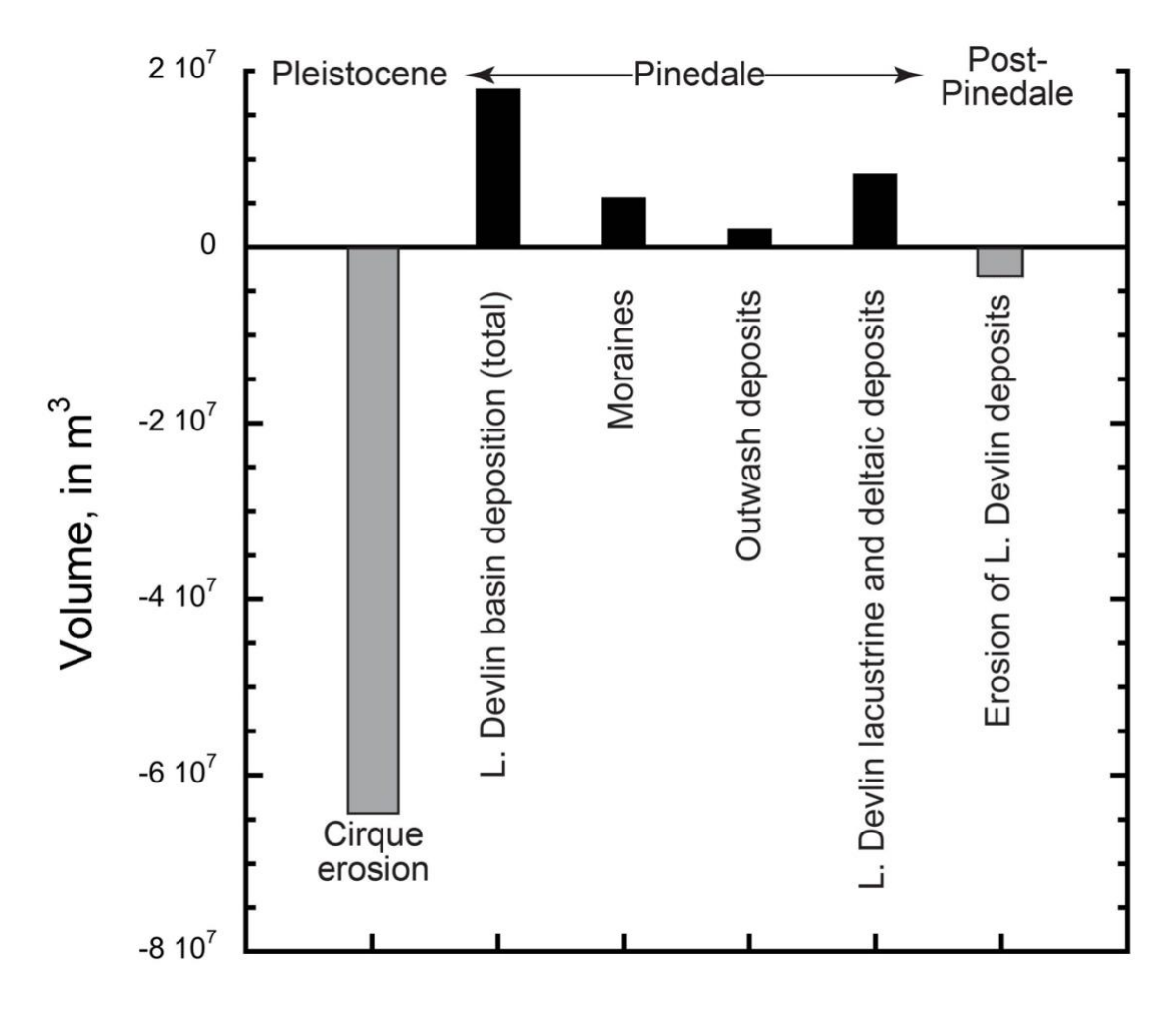
1025 Fig. 2



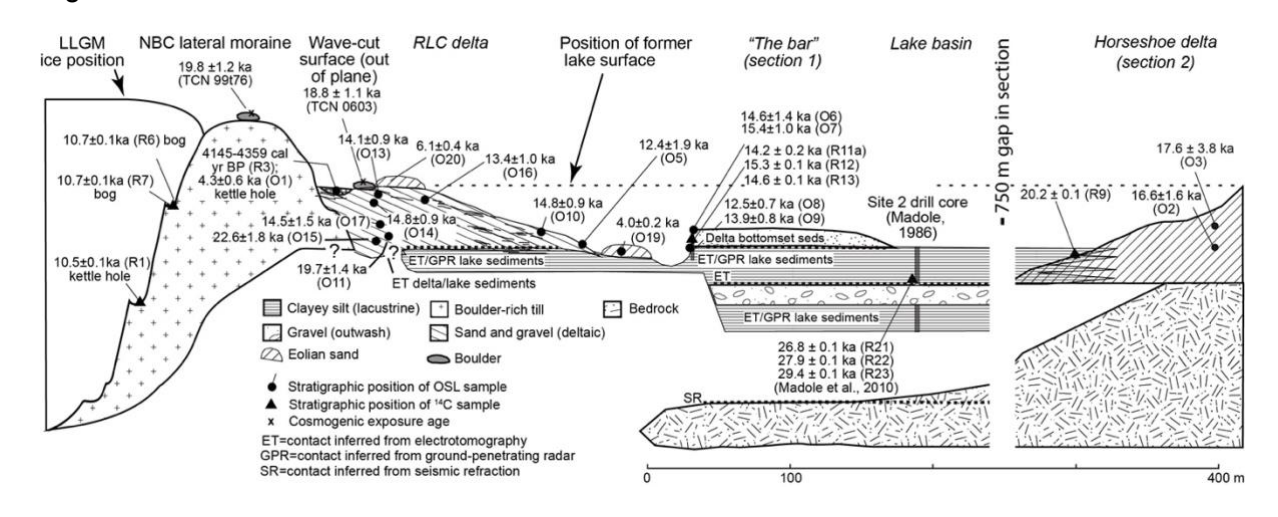




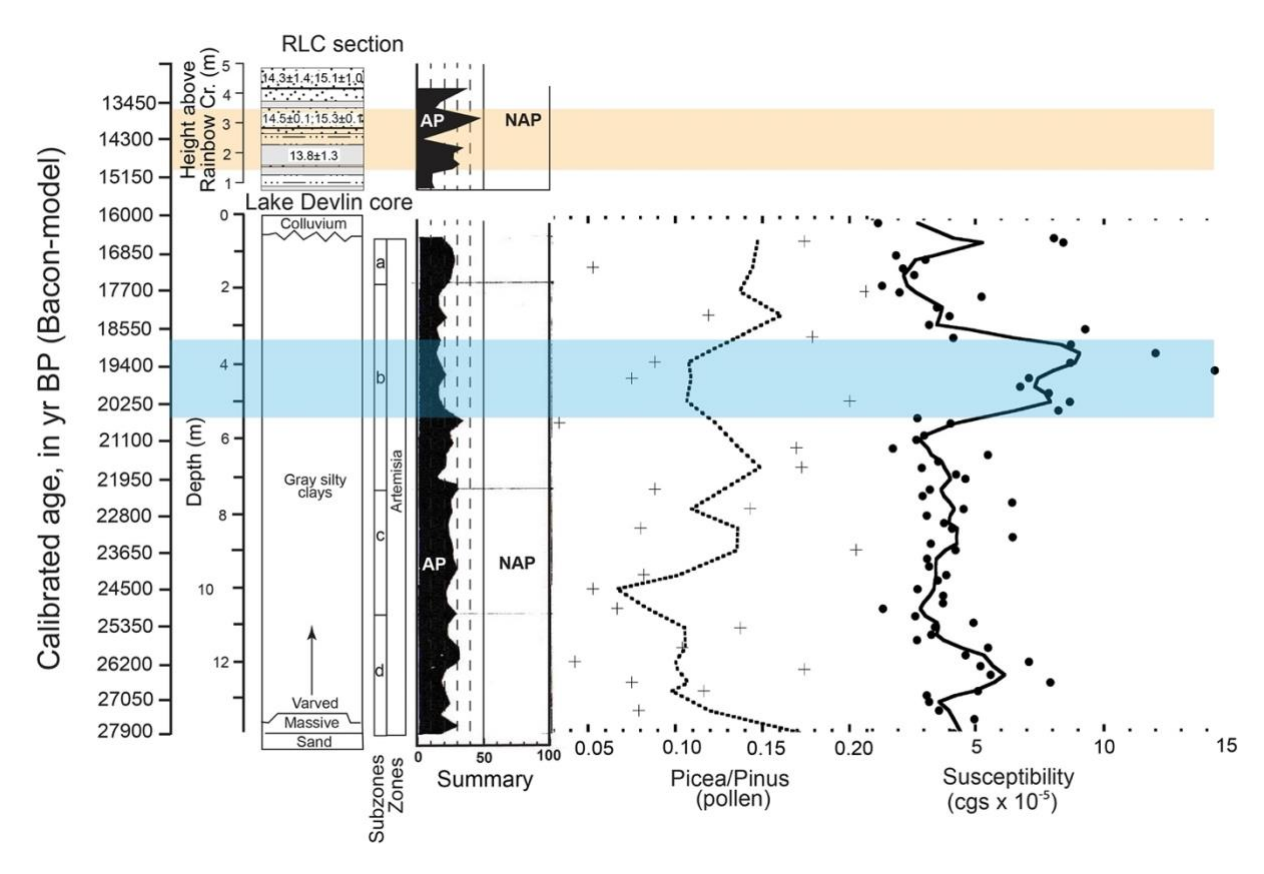




1034



1037 Fig. 8



1038

#### TABLE 1. SUMMARY OF DEPOSIT DATES AND EXPOSURE AGES, LAKE DEVLIN 1041

Sample number	Material	Lab no.	Date type	Age in ka <sup>1</sup>	cal yr BP ± 2	Median Probability age, yr	Location and comments
R1	Peat	Beta235293	Radiocarbon	9.31±0.08	10258 - 10693	10501	Kettle hole, N. Boulder Cr. valley
R2	Charcoal	Beta235294	Radiocarbon	0.25±0.04	264 - 331	296	Kettle hole, N. Boulder Cr. valley
R3	Charcoal	Beta-235295	Radiocarbon	3.83±0.04	4145 - 4359	4233	Kettle hole on terrace
R4	Charcoal	Beta235296	Radiocarbon	0.12±0.04	8 - 152	120	Kettle hole on terrace
R5	Peat	Beta235297	Radiocarbon	9.13±0.06	10197 - 10433	10302	Bog, N. Boulder Cr. Valley
R6	Peat	Beta235298	Radiocarbon	9.48±0.04	10580 - 10803	10728	Bog, N. Boulder Cr. Valley
R7	Peat	Beta235299	Radiocarbon	9.48±0.04	10580 - 10803	10728	Bog, N. Boulder Cr. Valley
R8	Peat	Beta235300	Radiocarbon	5.61±0.04		6376	
R9	Seed	Beta245664	Radiocarbon	16.72±0.06	6303 - 6454		N. Boulder Cr. Valley Horseshoe Cr. delta
R10		DIC2199		13.59±0.83	20013 - 20412	20222	
	Dispersed OM		Radiocarbon		13996 - 18309	16332	Horseshoe Cr. delta Rainbow Cr. delta
R11a³	Dispersed OM	GaK4834	Radiocarbon	12.18±0.24	13592 - 15045	14234	
R11b³	Dispersed OM	DIC2271	Radiocarbon	12.91±0.27	14771 - 16216	15406	Rainbow Cr. delta
R12	Seed	Beta242308	Radiocarbon	12.81±0.07	15092 - 15553	15294	Rainbow Cr. delta
R13	Seed	Beta224421	Radiocarbon	12.43±0.04	14292 - 14901	14562	Rainbow Cr. delta
R14 <sup>3</sup>	Dispersed OM	DIC865	Radiocarbon	15.23±0.31	18175 - 18914	18513	Core from lake bottom seds.
R15 <sup>3</sup>	Dispersed OM	DIC866	Radiocarbon	18.62±0.30	21886 - 23166	22565	Core from lake bottom seds.
R16 <sup>3</sup>	Dispersed OM	DIC868	Radiocarbon	17.46±1.0	18810 - 23348	21122	Core from lake bottom seds.
R17 <sup>3</sup>	Dispersed OM	DIC869	Radiocarbon	21.73±1.1	23683 - 28096	25936	Core from lake bottom seds.
R18 <sup>3</sup>	Dispersed OM	DIC870	Radiocarbon	22.40±1.15	24134 - 28993	26623	Core from lake bottom seds.
R19 <sup>3</sup>	Dispersed OM	DIC871	Radiocarbon	22.04±0.78	24590 - 27782	26318	Core from lake bottom seds.
R20 <sup>3</sup>	Dispersed OM	DIC574	Radiocarbon	21.18±2.86		25130	Core from lake bottom seds.
					18793 - 31091		
R21 <sup>4</sup>	Chironomid material	Aeon-247	Radiocarbon	22.46±0.09	26428 - 27067	26756	Core from lake bottom seds.
R22 <sup>4</sup>	Chironomid material	Aeon-246	Radiocarbon	23.83±0.08	27742 - 28185	27906	Core from lake bottom seds.
R23 <sup>4</sup>	Chironomid material	WW-6078	Radiocarbon	25.13±0.11	29142 - 29809	29416	Core from lake bottom seds.
01	Eolian sand	Risø 085401	OSL	4.3 ± 0.6			Kettle hole on terrace
O2 O3	Deltaic sands Deltaic sands	Risø 085402 Risø 085403	OSL OSL	16.6 ± 1.6 17.6 ± 3.8			Horseshoe Cr. delta Horseshoe Cr. delta
04	Glaciofluvial	Risø 085404	OSL	45.0 ± 4.0			N. Boulder Cr. valley terrace deposit
05	Fluvial	Risø 085405	OSL	12.4 ± 1.9			Slack water deposit
O6	Deltaic sands	Risø 065401	OSL	14.6 ± 1.4			"The bar" (top)
07	Deltaic sands	Risø 065402	OSL	15.4 ± 1.0			"The bar" (top)
O8	Deltaic sands	Risø 065403	OSL	12.5 ± 0.7			"The bar" (lower)
09	Deltaic sands	Risø 065404	OSL	13.9 ± 0.8			"The bar" (lower)
O10	Deltaic sands	Risø 065405	OSL	14.8 ± 0.9			Rainbow Cr. delta top
011	Deltaic sands	Risø 065406	OSL	19.7 ± 1.4			Rainbow Cr. delta lower, western exposure
012	Eolian sand	Risø 065407	OSL	8.1 ± 1.1			Deposited on wave cut surface 100 m west of "the bar"
013	Deltaic sands	Risø 065408	OSL	14.1 ± 0.9			Rainbow Cr. delta top
014	Deltaic sands	Risø 065409	OSL	14.8 ± 0.9			Rainbow Cr. delta middle
015	Deltaic sands	Risø 065410	OSL	22.6 ± 1.8			Rainbow Cr. delta base
016	Deltaic sands	Risø 065411	OSL	13.4 ± 1.0			Rainbow Cr. delta top
017	Deltaic sands	Risø 065412	OSL	14.5 ± 1.5			Rainbow Cr. delta middle
O18 O19	Deltaic sands  Eolian sand	Risø 065413 Risø 065414	OSL	16.2 ± 1.0 4.0 ± 0.2			Rainbow Cr. delta middle Sand sheet on erosional valley of
O20	Eolian sand	Risø 065415	OSL	6.1 ± 0.4			Rainbow Cr. Eolian deposited on wave-cut surface
							Pinedale lateral moraine (sampled an
99t76 99t76	<sup>10</sup> Be boulder exposure age	BE11711 AL7160	Cosmogenic	19.8 ± 1.2			prepared by T. Schildgen) Pinedale lateral moraine (sampled an
DC0603	<sup>26</sup> Al boulder exposure age <sup>10</sup> Be boulder exposure age		Cosmogenic				prepared by T. Schildgen)  Boulder exposed on wave-cut surface
DC0604	<sup>10</sup> Be boulder exposure age		Cosmogenic Cosmogenic	18.0 ± 1.1 11.1 ± 0.7			Outburst boulder deposit, age does no
TCU1	<sup>10</sup> Be bedrock exposure age	BE30866	Cosmogenic	23.5 ± 1.4			account for snow shielding  Exposure age for ice retreat?
TCU2	<sup>10</sup> Be bedrock exposure age		Cosmogenic	22.3 ± 1.3			Exposure age for ice retreat?
TCU3	<sup>10</sup> Be boulder exposure age		Cosmogenic	35.2 ± 2.1			pre-Pinedale moraine
			_				
TCU4	<sup>10</sup> Be boulder exposure age		Cosmogenic Cosmogenic	51.5 ± 3.1 21.2 ± 1.3			pre-Pinedale moraine Exposure age for cliff face after a period of spallation
TCU6	<sup>10</sup> Be bedrock exposure age		Cosmogenic	20.5 ± 1.2			Exposure age for cliff face after a

<sup>1. &</sup>lt;sup>14</sup>C ages reported in kyr BP and calibrated YBP ± 2 sigma. Other ages are ka. Optically stimulated luminescence (OSL) ages measured on potassium feldspar. Cosmogenic exposure ages calculated using the Cronus calculator, v. 3 (https://hess.ess.washington.edu/math/v3/v3\_age\_in.html.) and reported using the global production rate and LsDn scaling ± external error. Accessed 12.22.21

2. Calibrated radiocarbon ages and median probability ages calculated using Calib. Rev8.2 (Reimer et al., 2020), accessed 8.29.21

<sup>3.</sup> Original data in Madole (1986)

<sup>4.</sup> Original data provided from Madole (2010)

<sup>5.</sup> Geologic relations suggest date is "too young" 6. Geologic relations suggest date is "too old"

#### **BASIN AND VICINITY**

1044

1045

1046

1043

### TABLE 2. CALCULATED VOLUMES AND EROSION RATES FOR FEATURES AND DEPOSITS IN THE LAKE DEVLIN BASIN

Feature or deposit	Area, in km²	Basis	Thickness or erosion depth, in m (maximum )	Thickness or erosion depth, in m (minimum)	Volume, upper limit, m <sup>3</sup>	Volume, lower limit, m <sup>3</sup>	Volume, calculation value, m <sup>3</sup>	Calculated erosion rate of area upgradient from deposit, cm kyr <sup>-1</sup>	Notes
Rainbow cirque (erosion)	0.54	DEM model <sup>1</sup>	57.90	57.90		3.13E+07	3.13E+07	7.2	Rate assumes cirque was eroded over the past 800 kyr Rate assumes cirque was
Horseshoe cirque (erosion)	0.56	DEM model	58.00	58.00		3.25E+07	3.25E+07	7.3	eroded over the past 800 kyr
Rainbow moraine complex	1.07	DEM model	1.20	1.20	1.28E+06	1.28E+06	1.28E+06	3.1	Calculation assumes moraine formed during Pinedale time; catchment area is 2.55 km², 21.5% filled by a Pinedale glacier.
Horseshoe moraine complex	1.16	DEM model	3.75	3.75	4.35E+06	4.35E+06	4.36E+06	5.5	Calculation assumes moraine formed during Pinedale time; catchment area is 4.9 km², 11 to 45% filled by a Pinedale glacier (a thin tributary glacier may have covered 1.8 km²)
Horseshoe and Caribou outwash deposits	0.41	DEM and field mapping	5.00	3.00	2.05E+06	1.23E+06	2.05E+06	1.1	Contributing catchment area 11.8 km <sup>2</sup>
Deposition into L. Devlin, Pinedale total (lacustrine and deltaic) <sup>2</sup>	0.4	DEM and field mapping	30	20	1.20E+07	8.00E+06	7.00E+06	2.4	Catchment area 18 km <sup>2</sup> . Calculation value based on geologic mapping that indicates L. Devlin did not fill completely with sediment between delta areas
Total Pinedale sediment deposited in moraines, outwash and lacustrine deposits in L. Devlin catchment	18	Summation			1.97E+07	1.47E+07	1.72E+07	6.8	
L. Devlin Pinedale lacustrine deposits (preserved)	0.3	Estimate from field mapping and DEM	20.00	10.00	6.00E+06	3.00E+06	4.20E+06	·	Thickness estimated
Devlin outburst fan (preserved)	0.031	DEM and field mapping	5		2.00E+05	1.55E+05	1.78E+05		Erosion from moraine dam removed ~9.7E+05 m <sup>3</sup> of sediment
Erosion (post- Pinedale) of L. Devlin lacustrine deposits	0.3	DEM model	20.00	6.00	4.93E+06		3.45E+06	71.9	Graphic model value assuming L. Devlin was 70% filled with sediment

1047

1048

1049

1050

1051

1052

<sup>1</sup>Supplemental Material. [Supplemental data and figures for Dethier et al. Lake Devlin paper] Please

visit <a href="https://doi.org/10.1130/XXXX">https://doi.org/10.1130/XXXX</a> to access the supplemental material, and contact

editing@geosociety.org with any questions.

<sup>1.</sup> See Supplementary Materials
2. Rainbow + Horseshoe deta volume between 1.5 and 5.5 x10<sup>5</sup> m<sup>3</sup>; 1.8 x10<sup>5</sup> m<sup>3</sup> used in calculation; erosion of regolith on wave cut surface 6.4 x 10<sup>5</sup> m<sup>3</sup>; minimum value from area ~ 0.068 km<sup>2</sup>